Open access • Journal Article • DOI:10.1016/J.COMPOSITESB.2017.09.054

Size-dependent vibration of bi-directional functionally graded microbeams with arbitrary boundary conditions — Source link

Luan C. Trinh, Luan C. Trinh, Thuc P. Vo, Thuc P. Vo ...+3 more authors

Institutions: Northumbria University, Ho Chi Minh City University of Technology, Duy Tan University, La Trobe University ...+1 more institutions

Published on: 01 Feb 2018 - Composites Part B-engineering (Elsevier)

Topics: Timoshenko beam theory

Size-dependent vibration of bi-directional functionally graded microbeams with arbitrary boundary conditions

Luan C. Trinh [a,b], Thuc P. Vo [a,d*], Huu-Tai Thai [c], Trung-Kien Nguyen [b]

[a] Department of Mechanical and Construction Engineering, Northumbria University, Ellison Place, Newcastle upon Tyne NE1 8ST, UK

[b] Faculty of Civil Engineering, Ho Chi Minh City University of Technology and Education, 1 Vo Van Ngan Street, Thu Duc District, Ho Chi Minh City, Vietnam.

[c] School of Engineering and Mathematical Sciences, La Trobe University, Bundoora, VIC 3086, Australia

[d] Institute of Research and Development, Duy Tan University, 03 Quang Trung, Da Nang, Vietnam

Abstract

In this paper, the free vibration behaviour of bi-dimensional functionally graded (BDFG) microbeams under arbitrary boundary conditions (BCs) is studied. Based on the frame work of the modified couple stress theory and Hamilton's principle, governing equations of motion are developed for the BDFG microbeams using a quasi-3D theory. The formula then can be reduced to a higher-order beam theory (HOBT) of conventional functionally graded (FG) microbeams with the material properties varying along the thickness direction only. Two types of BDFG microbeams with different patterns of material volume distribution are considered. The material properties used in this study are assumed to vary exponentially along both longitudinal and thickness directions of microbeams. Based on the state-space concept, the governing equations are solved for natural frequencies and vibration mode shapes of microbeams under various BCs. The effects of material distribution, geometric parameters and BCs are also investigated to examine the size-dependent behaviour of BDFG microbeams.

Keywords: Bi-directional functionally graded microbeam; state-space based solution; modified couple stress theory; quasi-3D theory.

* Corresponding author. Tel.: +44 (0) 191 243 7856

E-mail address: thuc.vo@northumbria.ac.uk (Thuc P. Vo).

1. Introduction

Functionally graded materials (FGMs) are a class of composite structures formed by changing the material properties in the desired directions. The gradation process of this kind of materials can create the industrial products with smooth and continuous properties, hence avoids the stress concentration, cracking and delamination phenomena occurred in conventional composites. These striking features appeal the researchers in developing the advanced theories and analysis methods to predict more precisely the behaviours of FG materials/structures. Furthermore, recent development in technology requires the understanding in even micro-/nano-scale structures, which is pushing the research for the behaviours of these small scales. There are many approaches analysing the size-dependent behaviours of structures including the molecular dynamics simulation, molecular-continuum combinations and non-classical continuum methods. Among them, the third approach has been utilised expansively due to its computational efficiency and the possibility of linking between small- and macro- structures. Within the non-classical continuum approach, the modified couple stress theory (MCST), which was developed by Yang et al. [1] by modifying the classical couples stress theory [2-5], is advantageous since it requires only one additional material length scale parameter together with two from the classical continua. This feature was presented by the theoretical framework in [1], which proved that the antisymmetric part of curvature does not appear explicitly in the strain energy.

One of the earliest work on the application of MCST was to analyse the bending behaviour of an epoxy cantilever beam by Park and Gao [6] based on Bernoulli-Euler theory, which is widely known as the classical beam theory (CBT). Kong et al. [7] compared the variation of natural frequencies of the cantilever and simply supported homogeneous beams. Xia et al. [8] studied the static, post-buckling and free vibration behaviours of an epoxy beams considering geometric nonlinearity. It is worth noting that in the CBT, the cross-section is assumed to be flat and perpendicular to the neutral axis as deformed, which actually neglects the shear deformation effect. This results in the stiffer behaviours compared to the real working order of structures. The first-order beam theory (FOBT) was then developed to include the shear effect in analysing the structural behaviours. Using the FOBT, Ma et al. [9] examined the static

and free vibration behaviours of simply supported epoxy beams. Asghari et al. [10] obtained the Navier solution for static and vibration behaviours of cantilever FG beams by the CBT and then developed this model to the FOBT and von-Karman strain formulation for a simply supported homogeneous beams. Using the differential quadrature method, Ke and Wang [11] studied the dynamic stability of FG beams under the hinged and clamped supports. Ke et al. [12] also incorporated the geometric nonlinearity effects in the free vibration of FG beams. Dehrouyeh-Semnani et al. [13] investigated the free vibration of geometrically imperfect FG beams under various BCs based on the Rayleigh-Ritz's method. Reddy [14] examined the static bending, vibration and buckling behaviours of simply supported FG beams using both CBT and FOBT, which included the geometric nonlinearity effect. Using Navier solution, Simsek et al. [15] studied static bending behaviours of FG beams. Kahrobaiyan et al. [16] developed a FOBT beam element and applied to the cantilever FG beams under a concentrated load and a pull-in voltage. Thai et al. [17] studied the static, vibration and buckling behaviours of FG sandwich beams without a shear correction factor. They computed the transverse shear force and shear stress by using the equilibrium equations. Nateghi and Salamat-talab [18] included the thermal effect in analysing the free vibration and buckling behaviours of FG beams using both CBT and FOBT. Akgoz and Civalek [19] utilised the Rayleigh-Ritz solution to study the free vibration of axially graded tapered beams. In the FOBT, the cross-section is still assumed to be flat while loaded, which violates the free shear stress conditions at the top and bottom surfaces, and hence a shear correction factor is needed. This leads to the proposition of the third-order beam theory (TBT), higher-order beam deformation theories (HOBT) and quasi-3D theories. The effectiveness of these theories dealing with macro structures can be found in some recent contributions [20-29]. As regarded the micro scales, Nateghi et al. [30] applied the generalized differential quadrature method (GDQM) to examine the size-dependent buckling behaviour of FG beams using the CBT, FOBT and TBT. Salamat-talab et al. [31] presented an analytical solution for the static and free vibration behaviours of simply supported beams. Ansari et al. [32] developed a general strain gradient theory using the FOBT, which comprises the MCST, in analysing the bending, vibration and buckling of FG beams by applying the GDQM. Sahmani and Ansari [33] also extended the solutions of

buckling behaviour for the TBT with the inclusion of the thermal environment effect. Mohammad-Abadi and Daneshmehr [34] considered the buckling of FG beams under the CBT, FOBT and TBT. Simsek and Reddy [35] analysed bending and vibration behaviours, as well as buckling responses of FG beams with the inclusion of elastic Pasternak medium based on various HOBTs. Akgoz and Civalek [36, 37] employed a sinusoidal shear deformation to study the static and buckling behaviours, and the thermo-mechanical buckling of FG beams embedded in Winkler elastic medium under the framework of general strain gradient theory. Darijani and Mohammadabadi [38] employed the refined fifth-order shear deformation model for static, vibration and buckling behaviours of FG beams. Al-Basyouni et al. [39] studied the bending and vibration of FG beams based on the neutral surface position and unified HOBTs. Arbind and Reddy [40] proposed nonlinear finite element models based on the CBT and FOBT to analyse the bending behaviour of FG beams. Arbind et al. [41] later expanded these models to TBT and included the analytical solution to verify the finite element models. Al-Basyouni et al. [39] utilised the neutral surface concept to analyse the bending and vibration behaviours of simply supported FG microbeams using the CBT, FOBT and sinusoidal beam theory. Trinh et al. [42] analysed static bending, vibration and buckling of simply supported beams using various shear deformation theories. A comprehensive review on the development of MCST models and other non-classical continua, such as non-local elasticity [43-51] and strain gradient [52-54] can be found in recent works by Romano et al. [48] and Thai et al. [55].

Recently, there have been some publications on the BDFG beams, in which the material properties can be tailored in both the longitudinal and thickness directions. Lu et al. [56] analysed the bending and thermal deformations of BDFG beams using a system of state-space equations on the combination of stress and displacement variables. Lezgy-Nazargah [57] studied the fully coupled thermo-mechanical static behaviour of BDFG beams using NURBS isogeometric finite element method. Simsek analysed the free and force vibration [58] and buckling [59] of BDFG beams under various BCs. Hao and Wei [60] studied the dynamic characteristics of BDFG beams using a FOBT model. Utilising the NURBS-based isogeometric method, Huynh et al. [61] analysed the free vibration of various types of BDFG beams.

Karamanlı [62] studied the bending behaviour of a BDFG beams using different shear deformation theories and the symmetric smoothed particle hydrodynamics method. He then expanded this solution for BDFG sandwich beams using a quasi-3D theory [63]. However, only few papers investigated the small-scale analysis of BDFG beams. Nejad and Hadi [64, 65] analysed bending and vibration of BDFG nanobeams. Nejad et al. [66] also studied the buckling behaviour of these beams. In their papers, they developed the Eringen's nonlocal theory based on the CBT model with the GDQM. Shafiei and Kazemi [67] studied the buckling behaviour of BDFG porous tapered nano-/micro-scale beams using the CBT. Shafiei et al. [68] also investigated the vibration of imperfect BDFG porous nano-/micro-beams using the FOBT. As far as the authors are aware, there is no study dealing with the BDFG microbeams with arbitrary boundary conditions using the HOBT and quasi-3D theories.

This paper presents a quasi-3D model which includes both the transverse shear and normal deformation effects for the free vibration of conventional FG and BDFG microbeams. The state-space method is applied to analytically solve the governing equations for natural frequencies and vibration mode shapes of microbeams for the first time. The HOBT can be also deduced from the present quasi-3D model as a special case by neglecting the normal stretching effect. The effect of material properties, geometric parameters and BCs on the free vibration behaviour of conventional and BDFG microbeams are discussed.

2. Theoretical formulation

2.1. BDFG materials

Consider a FG microbeam with its dimensions and coordinate shown in Fig. 1a. The typical material properties of BDFG microbeams are expressed as:

$$P(x,z)=e^{V_x(x)}P(z) \tag{1}$$

where $P(x,z)$ stands for Young's modulus $E(x,z)$ or mass density $\rho(x,z)$. Poisson's ratio is assumed to be constant [58, 61]. The material properties vary exponentially along the axial direction describing by $V_x(x)=n_x\left(\frac{x}{a}+\frac{1}{2}\right)$. $P(z)$ is the function governing the variation of

material properties across the thickness. Three types of FG beams are considered in this paper including:

Type A: $P(z)=(P_c-P_m)\left(\frac{1}{2}+\frac{z}{h}\right)^{n_z}+P_m$ (2a)

Type B [58]: $P(z)=P_0e^{V_z(z)}$, where $V_z(z)=n_z\left(\frac{z}{h}+\frac{1}{2}\right)$ (2b)

Type C [61]: $P(z)=P_0e^{V_z(z)}$, where $V_z(z)=\begin{cases}2n_z\frac{z}{h}\ \text{if z}\in\left[-\frac{h}{2};0\right]\\ -2n_z\frac{z}{h}\text{if z}\in\left[0;\frac{h}{2}\right]\end{cases}$ (2c)

where P_c and P_m are the material properties of ceramic and metal, and n_z is the power-law index in Type A. For Types B and C, P_0 is the based material properties, whilst n_x and n_z are the exponential indices in x and z directions, respectively. The variation of Young's modulus is illustrated in Fig. 1 for conventional FG microbeams $(n_x=0,n_z=2)$ and BDFG microbeams $(n_x=n_z=2)$.

2.2. Kinematics and constitutive relations

The displacement field which includes both transverse shear and normal deformation effects is assumed as follows [69, 70]:

$$u(x,z,t)=U(x,t)-z\frac{\partial W_b(x,t)}{\partial x}-f(z)\frac{\partial W_s(x,t)}{\partial x} \tag{3a}$$

$$w(x,z,t)=W_b(x,t)+W_s(x,t)+g(z)W_z(x,t) \tag{3b}$$

where U,W_b,W_s and W_z are the mid-plane displacements of the axial, bending, shear and stretching components. $f(z)=\frac{4}{3}\frac{z^3}{h^2}$ and $g(z)=1-\frac{df(z)}{dz}$ are the shape functions of the higher-order and stretching displacements. The non-zero strain components related to the above displacement field are obtained as:

$$\varepsilon_{xx}=\frac{\partial U}{\partial x}-z\frac{\partial^2 W_b}{\partial x^2}-f(z)\frac{\partial^2 W_s}{\partial x^2} \tag{4a}$$

$$\varepsilon_{zz}=\frac{\partial g(z)}{\partial z}W_z \tag{4b}$$

$$\gamma_{xz} = g(z)\left(\frac{\partial W_s}{\partial x} + \frac{\partial W_z}{\partial x}\right) \tag{4c}$$

The rotation vector is expressed as:

$$\theta_y = \frac{1}{2} curl\, u\big|_{\mathbf{e}_y} = -\frac{\partial W_b}{\partial x} - \frac{1}{2}\left[1 + \frac{\partial f(z)}{\partial z}\right]\frac{\partial W_s}{\partial x} - \frac{1}{2} g(z)\frac{\partial W_z}{\partial x} \tag{5a}$$

$$\theta_x = \theta_z = 0 \tag{5b}$$

Hence, the non-zero curvature components are given by:

$$\chi_{xy} = \frac{\partial \theta_x}{\partial y} + \frac{\partial \theta_y}{\partial x} = \frac{1}{2}\left\{-\frac{\partial^2 W_b}{\partial x^2} - \frac{1}{2}\left[1 + \frac{\partial f(z)}{\partial z}\right]\frac{\partial^2 W_s}{\partial x^2} - \frac{1}{2} g(z)\frac{\partial^2 W_z}{\partial x^2}\right\} \tag{6a}$$

$$\chi_{yz} = \frac{\partial \theta_z}{\partial y} + \frac{\partial \theta_y}{\partial z} = \frac{1}{4}\left[-\frac{\partial^2 f(z)}{\partial z^2}\frac{\partial W_s}{\partial x} - \frac{\partial g(z)}{\partial z}\frac{\partial W_z}{\partial x}\right] \tag{6b}$$

The linear elastic constitutive relations are expressed for the stress and deviatoric part of couple stress tensors as:

$$\begin{Bmatrix}\sigma_{xx}\\ \sigma_{zz}\\ \sigma_{xz}\end{Bmatrix} = \begin{bmatrix} Q_{11} & Q_{13} & 0\\ & Q_{33} & 0\\ sym. & & Q_{66}\end{bmatrix}\begin{Bmatrix}\varepsilon_{xx}\\ \varepsilon_{zz}\\ \gamma_{xz}\end{Bmatrix} \tag{7a}$$

$$\begin{Bmatrix}m_{yz}\\ m_{xy}\end{Bmatrix} = 2l^2\mu\begin{Bmatrix}\chi_{yz}\\ \chi_{xy}\end{Bmatrix} \tag{7b}$$

where $Q_{11} = Q_{33} = \frac{E_0 e^{V_x(x)+V_z(z)}}{1-\upsilon^2}, Q_{13} = \frac{\upsilon E_0 e^{V_x(x)+V_z(z)}}{1-\upsilon^2}, Q_{66} = \frac{E_0 e^{V_x(x)+V_z(z)}}{2(1+\upsilon)}$, l is the material length scale parameter [1]. The value of l can be determined from experiments, e.g. $l = 17.6\mu m$ for homogeneous epoxy beams [54]. By substituting Eqs. (4) and (6) into Eq. (7), the stress and deviatoric part of couple stress tensors are rewritten in terms of displacement components as:

$$\begin{Bmatrix}\sigma_{xx}\\ \sigma_{zz}\\ \sigma_{xz}\end{Bmatrix} = \begin{bmatrix} Q_{11} & Q_{13} & 0\\ & Q_{33} & 0\\ sym. & & Q_{66}\end{bmatrix}\begin{Bmatrix}\dfrac{\partial U}{\partial x} - z\dfrac{\partial^2 W_b}{\partial x^2} - f(z)\dfrac{\partial^2 W_s}{\partial x^2}\\ \dfrac{\partial g(z)}{\partial z} W_z\\ g(z)\left(\dfrac{\partial W_s}{\partial x} + \dfrac{\partial W_z}{\partial x}\right)\end{Bmatrix} \tag{8a}$$

$$\begin{Bmatrix} m_{yz} \\ m_{xy} \end{Bmatrix} = 2l^2 Q_{66} \begin{Bmatrix} \frac{1}{4}\left(-\frac{\partial^2 f(z)}{\partial z^2}\frac{\partial W_s}{\partial x} - \frac{\partial g(z)}{\partial z}\frac{\partial W_z}{\partial x} \right) \\ \frac{1}{2}\left[-\frac{\partial^2 W_b}{\partial x^2} - \frac{1}{2}\left(1+\frac{\partial f(z)}{\partial z}\right)\frac{\partial^2 W_s}{\partial x^2} - \frac{1}{2}g(z)\frac{\partial^2 W_z}{\partial x^2} \right] \end{Bmatrix} \tag{8b}$$

2.3. Governing equations

Hamilton's principle is employed to obtain the equations of motion:

$$\int_{t_1}^{t_2} (\delta\Pi - \delta K)\, dt = 0 \tag{9}$$

where $\delta\Pi$ and δK denote the variation of strain and kinetic energy of the microbeam. The variation of the strain energy is written in terms of displacements as:

$$\delta\Pi = \int_{-a/2}^{a/2}\int_{-h/2}^{h/2} \left(\sigma_{ij}\delta\varepsilon_{ij} + m_{ij}\delta\chi_{ij}\right) dz dx$$

$$= \int_{-a/2}^{a/2}\int_{-h/2}^{h/2} \left[\sigma_{xx}\delta\varepsilon_{xx} + \sigma_{zz}\delta\varepsilon_{zz} + \sigma_{xz}\delta\gamma_{xz} + 2m_{xy}\delta\chi_{xy} + 2m_{yz}\delta\chi_{yz}\right] dz dx$$

$$= \int_{-a/2}^{a/2} \left[e^{V_x(x)}\left(N_{xx}\frac{\partial\delta U}{\partial x} - M_{xx}\frac{\partial^2\delta W_b}{\partial x^2} - P_{xx}\frac{\partial^2\delta W_s}{\partial x^2} \right) + e^{V_x(x)} O_{zz}\delta W_z \right.$$

$$+ e^{V_x(x)} Q_{xz}\left(\frac{\partial\delta W_s}{\partial x} + \frac{\partial\delta W_z}{\partial x} \right) - \frac{1}{2} e^{V_x(x)} X_{yz}\left(\frac{\partial\delta W_s}{\partial x} + \frac{\partial\delta W_z}{\partial x} \right)$$

$$\left. - e^{V_x(x)} R_{xy}\frac{\partial^2\delta W_b}{\partial x^2} - e^{V_x(x)} R_{xy}\frac{\partial^2\delta W_s}{\partial x^2} - e^{V_x(x)} S_{xy}\frac{\partial^2\delta W_s}{\partial x^2} - e^{V_x(x)} T_{xy}\frac{\partial^2\delta W_z}{\partial x^2} \right] dx \tag{10}$$

where the stress resultants are expressed as:

$$(N_{xx}, M_{xx}, P_{xx}) = \int_{-h/2}^{h/2} (1, z, f)\frac{E(z)}{1-\upsilon^2}\left[\frac{\partial U}{\partial x} - z\frac{\partial^2 W_b}{\partial x^2} - f(z)\frac{\partial^2 W_s}{\partial x^2} + W_z \right] dz \tag{11a}$$

$$O_{zz} = \int_{-h/2}^{h/2} \frac{\partial g}{\partial z}\frac{E(z)}{1-\upsilon^2} W_z dz \tag{11b}$$

$$Q_{xz} = \int_{-h/2}^{h/2} g\frac{E(z)}{2(1+\upsilon)}\left(\frac{\partial W_s}{\partial x} + \frac{\partial W_z}{\partial x} \right) dz \tag{11c}$$

$$\left(R_{xy}, S_{xy}, T_{xy}, X_{yz}\right) = \int_{-h/2}^{h/2} \left(1, \frac{\partial f}{\partial z}, g, \frac{\partial^2 f}{\partial z^2}\right) l^2 \frac{E(z)}{1+\upsilon}\left[-\frac{\partial^2 W_b}{\partial x^2} - \frac{1}{2}\left(1+\frac{\partial f}{\partial z}\right)\frac{\partial^2 W_s}{\partial x^2} - \frac{1}{2} g\frac{\partial^2 W_z}{\partial x^2} \right] dz \tag{11d}$$

The stress resultants can be rewritten as:

$$N_{xx} = A_{11}\frac{\partial U}{\partial x} - B_{11}\frac{\partial^2 W_b}{\partial x^2} - B_{11}^s\frac{\partial^2 W_s}{\partial x^2} + K_{13}W_z \tag{12a}$$

$$M_{xx} = B_{11}\frac{\partial U}{\partial x} - D_{11}\frac{\partial^2 W_b}{\partial x^2} - D_{11}^s\frac{\partial^2 W_s}{\partial x^2} + L_{13}W_z \tag{12b}$$

$$P_{xx} = B_{11}^s\frac{\partial U}{\partial x} - D_{11}^s\frac{\partial^2 W_b}{\partial x^2} - H_{11}\frac{\partial^2 W_s}{\partial x^2} + L_{13}^s W_z \tag{12c}$$

$$O_{zz} = K_{13}\frac{\partial U}{\partial x} - L_{13}\frac{\partial^2 W_b}{\partial x^2} - L_{13}^s\frac{\partial^2 W_s}{\partial x^2} + Z_{33}W_z \tag{12d}$$

$$Q_{xz} = A_{55}^s\left(\frac{\partial W_s}{\partial x} + \frac{\partial W_z}{\partial x}\right) \tag{12e}$$

$$R_{xy} = -A_m\frac{\partial^2 W_b}{\partial x^2} - \frac{1}{2}\left(A_m + B_m\right)\frac{\partial^2 W_s}{\partial x^2} - \frac{1}{2}E_m\frac{\partial^2 W_z}{\partial x^2} \tag{12f}$$

$$S_{xy} = -B_m\frac{\partial^2 W_b}{\partial x^2} - \frac{1}{2}\left(B_m + C_m\right)\frac{\partial^2 W_s}{\partial x^2} - \frac{1}{2}D_m\frac{\partial^2 W_z}{\partial x^2} \tag{12g}$$

$$T_{xy} = -E_m\frac{\partial^2 W_b}{\partial x^2} - \frac{1}{2}\left(E_m + D_m\right)\frac{\partial^2 W_s}{\partial x^2} - \frac{1}{2}F_m\frac{\partial^2 W_z}{\partial x^2} \tag{12h}$$

$$X_{yz} = -\frac{1}{2}H_m\frac{\partial W_s}{\partial x} + \frac{1}{2}H_m\frac{\partial W_z}{\partial x} \tag{12i}$$

where

$$\left(A_{ij}, B_{ij}, B_{ij}^s, D_{ij}, D_{ij}^s, H_{ij}, Z_{ij}\right) = \int_{-h/2}^{h/2}\left[1, z, f, z^2, fz, f^2, \left(\frac{dg}{dz}\right)^2\right]\frac{E(z)}{1-\upsilon^2}dz \tag{13a}$$

$$A_{ij}^s = \int_{-h/2}^{h/2} g^2\frac{E(z)}{2(1+\upsilon)}dz \tag{13b}$$

$$\left(K_{ij}, L_{ij}, L_{ij}^s, Z_{ij}\right) = \int_{-h/2}^{h/2}\left(1, z, f, \frac{\partial g}{\partial z}\right)\frac{\partial g}{\partial z}\frac{E(z)}{2(1+\upsilon)}dz \tag{13c}$$

$$\left[A_m, B_m, C_m, D_m, E_m, F_m, G_m, H_m\right] = \int_{-h/2}^{h/2}\frac{E(z)}{1+\upsilon}l^2\left[1, \frac{\partial f}{\partial z}, \left(\frac{\partial f}{\partial z}\right)^2, \frac{\partial f}{\partial z}g, g, g^2, \frac{\partial g}{\partial z}, \left(\frac{\partial g}{\partial z}\right)^2\right]dz \tag{13d}$$

The variation of the kinetic energy is presented by:

$$\delta K = \int_{-a/2}^{a/2}\int_{-h/2}^{h/2}\rho(x,z)\left(\dot{u}_1\delta\dot{u}_1 + \dot{u}_3\delta\dot{u}_3\right)dzdx$$

$$= \int_{-a/2}^{a/2}\left\{e^{V_x(x)}I_0\left[\dot{U}\delta\dot{U} + \left(\dot{W}_b + \dot{W}_s\right)\delta\left(\dot{W}_b + \dot{W}_s\right)\right] + e^{V_x(x)}J_0\left[\left(\dot{W}_b + \dot{W}_s\right)\delta\dot{W}_z + \dot{W}_z\delta\left(\dot{W}_b + \dot{W}_s\right)\right]\right.$$

$$-e^{V_x(x)}I_1\left(\dot{U}\frac{\partial\delta\dot{W}_b}{\partial x}+\frac{\partial\dot{W}_s}{\partial x}\delta\dot{U}\right)+e^{V_x(x)}I_2\frac{\partial\dot{W}_b}{\partial x}\frac{\partial\delta\dot{W}_b}{\partial x}-e^{V_x(x)}J_1\left(\dot{U}\frac{\partial\delta\dot{W}_s}{\partial x}+\frac{\partial\dot{W}_s}{\partial x}\delta\dot{U}\right)$$

$$+e^{V_x(x)}K_2\frac{\partial\dot{W}_s}{\partial x}\frac{\partial\delta\dot{W}_s}{\partial x}+e^{V_x(x)}J_2\left(\frac{\partial\dot{W}_b}{\partial x}\frac{\partial\delta\dot{W}_s}{\partial x}+\frac{\partial\dot{W}_s}{\partial x}\frac{\partial\delta\dot{W}_b}{\partial x}\right)+e^{V_x(x)}K_0\dot{W}_z\delta\dot{W}_z\Bigg\}dx \tag{14}$$

where

$$\left(I_0,I_1,I_2,J_0,J_1,J_2,K_0,K_2\right)=\int_{-h/2}^{h/2}\left(1,z,z^2,g,f,zf,g^2,f^2\right)\rho(z)dz \tag{15}$$

Substituting Eqs. (10) and (14) into Eq. (9), integrating by parts and gathering the coefficients of $\delta U,\delta W_b,\delta W_s$ and δW_z, and considering that $V_x(x)=n_x\left(\frac{x}{a}+\frac{1}{2}\right)$, the equations of motion can be obtained:

$$\frac{\partial N_x}{\partial x}+\frac{n_x}{a}N_x=I_0\ddot{U}-I_1\frac{\partial\delta\ddot{W}_b}{\partial x}-J_1\frac{\partial\ddot{W}_s}{\partial x} \tag{16a}$$

$$\frac{\partial^2M_x}{\partial x^2}+2\frac{n_x}{a}\frac{\partial M_x}{\partial x}+\left(\frac{n_x}{a}\right)^2M_x+\frac{\partial^2R_{xy}}{\partial x^2}+2\frac{n_x}{a}\frac{\partial R_{xy}}{\partial x}+\left(\frac{n_x}{a}\right)^2R_{xy}$$

$$=I_0\left(\ddot{W}_b+\ddot{W}_s\right)+J_0\ddot{W}_z+\left(\frac{n_x}{a}I_1\ddot{U}+I_1\frac{\partial\ddot{U}}{\partial x}\right)-\left(\frac{n_x}{a}I_2\frac{\partial\ddot{W}_b}{\partial x}+I_2\frac{\partial^2\ddot{W}_b}{\partial x^2}\right)-\left(\frac{n_x}{a}J_2\frac{\partial\ddot{W}_s}{\partial x}+J_2\frac{\partial^2\ddot{W}_s}{\partial x^2}\right) \tag{16b}$$

$$\frac{\partial^2P_x}{\partial x^2}+2\frac{n_x}{a}\frac{\partial P_x}{\partial x}+\left(\frac{n_x}{a}\right)^2P_x+\frac{\partial Q_{xz}}{\partial x}+\frac{n_x}{a}Q_{xz}+\frac{1}{2}\left[\frac{\partial^2R_{xy}}{\partial x^2}+2\frac{n_x}{a}\frac{\partial R_{xy}}{\partial x}+\left(\frac{n_x}{a}\right)^2R_{xy}\right]$$

$$+\frac{1}{2}\left[\frac{\partial^2S_{xy}}{\partial x^2}+2\frac{n_x}{a}\frac{\partial S_{xy}}{\partial x}+\left(\frac{n_x}{a}\right)^2S_{xy}\right]-\frac{1}{2}\left(\frac{\partial X_{yz}}{\partial x}+\frac{n_x}{a}X_{yz}\right)$$

$$=\left(\frac{n_x}{a}J_1\ddot{U}+J_1\frac{\partial\ddot{U}}{\partial x}\right)+I_0\left(\ddot{W}_b+\ddot{W}_s\right)+J_0\ddot{W}_z-\left(\frac{n_x}{a}K_2\frac{\partial\ddot{W}_s}{\partial x}+K_2\frac{\partial^2\ddot{W}_s}{\partial x^2}\right)-\left(\frac{n_x}{a}J_2\frac{\partial\ddot{W}_b}{\partial x}+J_2\frac{\partial^2\ddot{W}_b}{\partial x^2}\right) \tag{16c}$$

$$-O_{zz}+\frac{\partial Q_{xz}}{\partial x}+\frac{n_x}{a}Q_{xz}-\frac{1}{2}\left(\frac{\partial X_{yz}}{\partial x}+\frac{n_x}{a}X_{yz}\right)+\frac{1}{2}\left[\frac{\partial^2T_{xy}}{\partial x^2}+2\frac{n_x}{a}\frac{\partial T_{xy}}{\partial x}+\left(\frac{n_x}{a}\right)^2T_{xy}\right]=J_0\left(\ddot{W}_b+\ddot{W}_s\right)+K_0\ddot{W}_z \tag{16d}$$

The essential BCs are expressed as:

$$\delta\mathrm{W}_b:\frac{n_x}{a}M_x+\frac{\partial M_x}{\partial x}+\frac{n_x}{a}R_{xy}+\frac{\partial R_{xy}}{\partial x}=I_2\omega^2\frac{\partial W_b}{\partial x}+J_2\omega^2\frac{\partial W_s}{\partial x} \tag{17a}$$

$$\delta\frac{\partial\mathrm{W}_b}{\partial x}:M_x+R_{xy}=0 \tag{17b}$$

$$\delta\mathrm{W}_s:P_x+Q_{xz}-\frac{1}{2}X_{yz}+\frac{1}{2}\left(\frac{n_x}{a}R_{xy}+\frac{\partial R_{xy}}{\partial x}\right)+\frac{1}{2}\left(\frac{n_x}{a}S_{xy}+\frac{\partial S_{xy}}{\partial x}\right)=-J_1\omega^2U+K_2\omega^2\frac{\partial W_s}{\partial x}+J_2\omega^2\frac{\partial W_b}{\partial x} \tag{17c}$$

$$\delta \frac{\partial \mathrm{W}_s}{\partial x} : P_x + \frac{1}{2} R_{xy} + \frac{1}{2} S_{xy} = 0 \tag{17d}$$

$$\delta W_z : Q_{xz} - \frac{1}{2} X_{yz} + \frac{1}{2}\left(\frac{n_x}{a} T_{xy} + \frac{\partial T_{xy}}{\partial x} \right) = 0 \tag{17e}$$

$$\delta \frac{\partial \mathrm{W}_z}{\partial x} : T_{xy} = 0$$

The governing equations are expressed in terms of displacements as:

$$\left(A_{11} \frac{\partial^2 U}{\partial x^2} - B_{11} \frac{\partial^3 W_b}{\partial x^3} - B_{11}^s \frac{\partial^3 W_s}{\partial x^3} + K_{13} \frac{\partial W_z}{\partial x} \right) + \frac{n_x}{a} \left(A_{11} \frac{\partial U}{\partial x} - B_{11} \frac{\partial^2 W_b}{\partial x^2} - B_{11}^s \frac{\partial^2 W_s}{\partial x^2} + K_{13} W_z \right)$$

$$= -I_0 \omega^2 U + I_1 \omega^2 \frac{\partial W_b}{\partial x} + J_1 \omega^2 \frac{\partial W_s}{\partial x} \tag{18a}$$

$$B_{11} \frac{\partial^3 U}{\partial x^3} - D_{11} \frac{\partial^4 W_b}{\partial x^4} - D_{11}^s \frac{\partial^4 W_s}{\partial x^4} + L_{13} \frac{\partial^2 W_z}{\partial x^2} + 2 \frac{n_x}{a} \left(B_{11} \frac{\partial^2 U}{\partial x^2} - D_{11} \frac{\partial^3 W_b}{\partial x^3} - D_{11}^s \frac{\partial^3 W_s}{\partial x^3} + L_{13} \frac{\partial W_z}{\partial x} \right)$$

$$+ \left(\frac{n_x}{a} \right)^2 \left(B_{11} \frac{\partial U}{\partial x} - D_{11} \frac{\partial^2 W_b}{\partial x^2} - D_{11}^s \frac{\partial^2 W_s}{\partial x^2} + L_{13} W_z \right)$$

$$- A_m \frac{\partial^4 W_b}{\partial x^4} - \frac{1}{2}\left(A_m + B_m \right) \frac{\partial^4 W_s}{\partial x^4} - \frac{1}{2} E_m \frac{\partial^4 W_z}{\partial x^4} + 2 \frac{n_x}{a} \left(- A_m \frac{\partial^3 W_b}{\partial x^3} - \frac{1}{2}\left(A_m + B_m \right) \frac{\partial^3 W_s}{\partial x^3} - \frac{1}{2} E_m \frac{\partial^3 W_z}{\partial x^3} \right)$$

$$+ \left(\frac{n_x}{a} \right)^2 \left(- A_m \frac{\partial^2 W_b}{\partial x^2} - \frac{1}{2}\left(A_m + B_m \right) \frac{\partial^2 W_s}{\partial x^2} - \frac{1}{2} E_m \frac{\partial^2 W_z}{\partial x^2} \right)$$

$$= \left(-I_0 \omega^2 W_b - I_0 \omega^2 W_s \right) - J_0 \omega^2 W_z + \left(- \frac{n_x}{a} I_1 \omega^2 U - I_1 \omega^2 \frac{\partial U}{\partial x} \right)$$

$$+ \left(\frac{n_x}{a} I_2 \omega^2 \frac{\partial W_b}{\partial x} + I_2 \omega^2 \frac{\partial^2 W_b}{\partial x^2} \right) + \left(\frac{n_x}{a} J_2 \omega^2 \frac{\partial W_s}{\partial x} + J_2 \omega^2 \frac{\partial^2 W_s}{\partial x^2} \right) \tag{18b}$$

$$B_{11}^s \frac{\partial^3 U}{\partial x^3} - D_{11}^s \frac{\partial^4 W_b}{\partial x^4} - H_{11} \frac{\partial^4 W_s}{\partial x^4} + L_{13}^s \frac{\partial^2 W_z}{\partial x^2} + 2 \frac{n_x}{a} \left(B_{11}^s \frac{\partial^2 U}{\partial x^2} - D_{11}^s \frac{\partial^3 W_b}{\partial x^3} - H_{11} \frac{\partial^3 W_s}{\partial x^3} + L_{13}^s \frac{\partial W_z}{\partial x} \right)$$

$$+ \left(\frac{n_x}{a} \right)^2 \left(B_{11}^s \frac{\partial U}{\partial x} - D_{11}^s \frac{\partial^2 W_b}{\partial x^2} - H_{11} \frac{\partial^2 W_s}{\partial x^2} + L_{13}^s W_z \right) + A_{55}^s \left(\frac{\partial^2 W_s}{\partial x^2} + \frac{\partial^2 W_z}{\partial x^2} \right) + \frac{n_x}{a} A_{55}^s \left(\frac{\partial W_s}{\partial x} + \frac{\partial W_z}{\partial x} \right)$$

$$+ \frac{1}{2} \left\{ \begin{array}{l} - A_m \frac{\partial^4 W_b}{\partial x^4} - \frac{1}{2}\left(A_m + B_m \right) \frac{\partial^4 W_s}{\partial x^4} - \frac{1}{2} E_m \frac{\partial^4 W_z}{\partial x^4} + 2 \frac{n_x}{a} \left[- A_m \frac{\partial^3 W_b}{\partial x^3} - \frac{1}{2}\left(A_m + B_m \right) \frac{\partial^3 W_s}{\partial x^3} - \frac{1}{2} E_m \frac{\partial^3 W_z}{\partial x^3} \right] \\ + \left(\frac{n_x}{a} \right)^2 \left[- A_m \frac{\partial^2 W_b}{\partial x^2} - \frac{1}{2}\left(A_m + B_m \right) \frac{\partial^2 W_s}{\partial x^2} - \frac{1}{2} E_m \frac{\partial^2 W_z}{\partial x^2} \right] \end{array} \right\}$$

$$+\frac{1}{2}\left\{\begin{array}{l}\left[-B_m\frac{\partial^4 W_b}{\partial x^4}-\frac{1}{2}\left(B_m+C_m\right)\frac{\partial^4 W_s}{\partial x^4}-\frac{1}{2}D_m\frac{\partial^4 W_z}{\partial x^4}+2\frac{n_x}{a}\left[-B_m\frac{\partial^3 W_b}{\partial x^3}-\frac{1}{2}\left(B_m+C_m\right)\frac{\partial^3 W_s}{\partial x^3}-\frac{1}{2}D_m\frac{\partial^3 W_z}{\partial x^3}\right]\right.\\ \left.+\left(\frac{n_x}{a}\right)^2\left[-B_m\frac{\partial^2 W_b}{\partial x^2}-\frac{1}{2}\left(B_m+C_m\right)\frac{\partial^2 W_s}{\partial x^2}-\frac{1}{2}D_m\frac{\partial^2 W_z}{\partial x^2}\right]\right.\end{array}\right\}$$

$$+\frac{1}{4}H_m\left[\left(\frac{\partial^2 W_s}{\partial x^2}-\frac{\partial^2 W_z}{\partial x^2}\right)+\frac{n_x}{a}\left(\frac{\partial W_s}{\partial x}-\frac{\partial W_z}{\partial x}\right)\right]$$

$$=-J_1\omega^2\left(\frac{n_x}{a}U+\frac{\partial U}{\partial x}\right)-I_0\omega^2\left(W_b+W_s\right)-J_0\omega^2 W_z+K_2\omega^2\left(\frac{n_x}{a}\frac{\partial W_s}{\partial x}+\frac{\partial^2 W_s}{\partial x^2}\right)+J_2\omega^2\left(\frac{n_x}{a}\frac{\partial W_b}{\partial x}+\frac{\partial^2 W_b}{\partial x^2}\right) \quad (18c)$$

$$-K_{13}\frac{\partial U}{\partial x}+L_{13}\frac{\partial^2 W_b}{\partial x^2}+L_{13}^s\frac{\partial^2 W_s}{\partial x^2}-Z_{33}W_z+A_{55}^s\left(\frac{\partial^2 W_s}{\partial x^2}+\frac{\partial^2 W_z}{\partial x^2}\right)+\frac{n_x}{a}A_{55}^s\left(\frac{\partial W_s}{\partial x}+\frac{\partial W_z}{\partial x}\right)$$

$$+\frac{1}{2}H_m\left[\frac{\partial^2 W_s}{\partial x^2}-\frac{\partial^2 W_z}{\partial x^2}+\frac{n_x}{a}\left(\frac{\partial W_s}{\partial x}-\frac{\partial W_z}{\partial x}\right)\right]$$

$$+\frac{1}{2}\left\{\begin{array}{l}\left[-E_m\frac{\partial^4 W_b}{\partial x^4}-\frac{1}{2}\left(E_m+D_m\right)\frac{\partial^4 W_s}{\partial x^4}-\frac{1}{2}F_m\frac{\partial^4 W_z}{\partial x^4}+2\frac{n_x}{a}\left[-E_m\frac{\partial^3 W_b}{\partial x^3}-\frac{1}{2}\left(E_m+D_m\right)\frac{\partial^3 W_s}{\partial x^3}-\frac{1}{2}F_m\frac{\partial^3 W_z}{\partial x^3}\right]\right.\\ \left.+\left(\frac{n_x}{a}\right)^2\left[-E_m\frac{\partial^2 W_b}{\partial x^2}-\frac{1}{2}\left(E_m+D_m\right)\frac{\partial^2 W_s}{\partial x^2}-\frac{1}{2}F_m\frac{\partial^2 W_z}{\partial x^2}\right]\right.\end{array}\right\}$$

$$=-J_0\omega^2\left(W_b+W_s\right)-K_0\omega^2 W_z \quad (18d)$$

Using the state-space concept, the highest order derivatives of displacements are expressed in terms of other components as:

$$\frac{\partial^2 U}{\partial x^2}=a_1U+a_2\frac{\partial U}{\partial x}+a_3\frac{\partial W_b}{\partial x}+a_4\frac{\partial^2 W_b}{\partial x^2}+a_5\frac{\partial^3 W_b}{\partial x^3}+a_6\frac{\partial W_s}{\partial x}+a_7\frac{\partial^2 W_s}{\partial x^2}+a_8\frac{\partial^3 W_s}{\partial x^3}+a_9W_z+a_{10}\frac{\partial W_z}{\partial x} \quad (19a)$$

$$\frac{\partial^4 W_b}{\partial x^4}=r_1U+r_2\frac{\partial U}{\partial x}+r_3W_b+r_4\frac{\partial W_b}{\partial x}+r_5\frac{\partial^2 W_b}{\partial x^2}+r_6\frac{\partial^3 W_b}{\partial x^3}$$

$$+r_7W_s+r_8\frac{\partial W_s}{\partial x}+r_9\frac{\partial^2 W_s}{\partial x^2}+r_{10}\frac{\partial^3 W_s}{\partial x^3}+r_{11}W_z+r_{12}\frac{\partial W_z}{\partial x}+r_{13}\frac{\partial^2 W_z}{\partial x^2}+r_{14}\frac{\partial^3 W_z}{\partial x^3} \quad (19b)$$

$$\frac{\partial^4 W_s}{\partial x^4}=s_1U+s_2\frac{\partial U}{\partial x}+s_3W_b+s_4\frac{\partial W_b}{\partial x}+s_5\frac{\partial^2 W_b}{\partial x^2}+s_6\frac{\partial^3 W_b}{\partial x^3}$$

$$+s_7W_s+s_8\frac{\partial W_s}{\partial x}+s_9\frac{\partial^2 W_s}{\partial x^2}+s_{10}\frac{\partial^3 W_s}{\partial x^3}+s_{11}W_z+s_{12}\frac{\partial W_z}{\partial x}+s_{13}\frac{\partial^2 W_z}{\partial x^2}+s_{14}\frac{\partial^3 W_z}{\partial x^3} \quad (19c)$$

$$\frac{\partial^4 W_z}{\partial x^4}=t_1U+t_2\frac{\partial U}{\partial x}+t_3W_b+t_4\frac{\partial W_b}{\partial x}+t_5\frac{\partial^2 W_b}{\partial x^2}+t_6\frac{\partial^3 W_b}{\partial x^3}$$

$$+t_7W_s+t_8\frac{\partial W_s}{\partial x}+t_9\frac{\partial^2 W_s}{\partial x^2}+t_{10}\frac{\partial^3 W_s}{\partial x^3}+t_{11}W_z+t_{12}\frac{\partial W_z}{\partial x}+t_{13}\frac{\partial^2 W_z}{\partial x^2}+t_{14}\frac{\partial^3 W_z}{\partial x^3} \quad (19d)$$

The coefficients in Eq. (19) are given in the Appendix. The systems of Eq. (19) can be converted into a

matrix form using state-space approach as:

$$\frac{\partial \mathbf{U}(x)}{\partial x} = \mathbf{T}\mathbf{U}(x) \tag{20}$$

where the vector of variables is

$$\mathbf{U}(x) = \left\{ U, \frac{\partial U}{\partial x}, W_b, \frac{\partial W_b}{\partial x}, \frac{\partial^2 W_b}{\partial x^2}, \frac{\partial^3 W_b}{\partial x^3}, W_s, \frac{\partial W_s}{\partial x}, \frac{\partial^2 W_s}{\partial x^2}, \frac{\partial^3 W_s}{\partial x^3}, W_z, \frac{\partial W_z}{\partial x}, \frac{\partial^2 W_z}{\partial x^2}, \frac{\partial^3 W_z}{\partial x^3} \right\}^{'}; \tag{21}$$

and the non-zero components of matrix $\mathbf{T}$ are defined as:

$$\mathbf{T} = \begin{bmatrix}
0 & 1 & 0 & 0 & 0 & 0 & 0 & 0 & 0 & 0 & 0 & 0 & 0 & 0 \\
a_1 & a_2 & 0 & a_3 & a_4 & a_5 & 0 & a_6 & a_7 & a_8 & a_9 & a_{10} & 0 & 0 \\
0 & 0 & 0 & 1 & 0 & 0 & 0 & 0 & 0 & 0 & 0 & 0 & 0 & 0 \\
0 & 0 & 0 & 0 & 1 & 0 & 0 & 0 & 0 & 0 & 0 & 0 & 0 & 0 \\
0 & 0 & 0 & 0 & 0 & 1 & 0 & 0 & 0 & 0 & 0 & 0 & 0 & 0 \\
r_1 & r_2 & r_3 & r_4 & r_5 & r_6 & r_7 & r_8 & r_9 & r_{10} & r_{11} & r_{12} & r_{13} & r_{14} \\
0 & 0 & 0 & 0 & 0 & 0 & 0 & 1 & 0 & 0 & 0 & 0 & 0 & 0 \\
0 & 0 & 0 & 0 & 0 & 0 & 0 & 0 & 1 & 0 & 0 & 0 & 0 & 0 \\
0 & 0 & 0 & 0 & 0 & 0 & 0 & 0 & 0 & 1 & 0 & 0 & 0 & 0 \\
s_1 & s_2 & s_3 & s_4 & s_5 & s_6 & s_7 & s_8 & s_9 & s_{10} & s_{11} & s_{12} & s_{13} & s_{14} \\
0 & 0 & 0 & 0 & 0 & 0 & 0 & 0 & 0 & 0 & 0 & 1 & 0 & 0 \\
0 & 0 & 0 & 0 & 0 & 0 & 0 & 0 & 0 & 0 & 0 & 0 & 1 & 0 \\
0 & 0 & 0 & 0 & 0 & 0 & 0 & 0 & 0 & 0 & 0 & 0 & 0 & 1 \\
t_1 & t_2 & t_3 & t_4 & t_5 & t_6 & t_7 & t_8 & t_9 & t_{10} & t_{11} & t_{12} & t_{13} & t_{14}
\end{bmatrix} \tag{22}$$

A formal solution of Eq. (20) is given by:

$$\mathbf{U}(x) = \mathbf{e}^{\mathbf{T}x}\mathbf{K} \tag{23}$$

where $\mathbf{K}$ is a vector which can be solved from the BCs at $x = \pm a/2$ and $\mathbf{e}^{\mathbf{T}x}$ is of the form:

$$\mathbf{e}^{\mathbf{T}x} = \mathbf{E}\begin{bmatrix} e^{\lambda_1 x} & & 0 \\ & \ddots & \\ 0 & & e^{\lambda_{14} x} \end{bmatrix}\mathbf{E}^{-1} \tag{24}$$

where $\boldsymbol{\lambda}$ and $\mathbf{E}$ are the eigenvalues and columns of eigenvectors, respectively, associated with matrix $\mathbf{T}$. The BCs expressed in terms of displacement variables are described by:

Clamped (C): $U = W_b = \dfrac{\partial W_b}{\partial x} = W_s = \dfrac{\partial W_s}{\partial x} = W_z = \dfrac{\partial W_z}{\partial x} = 0$ (25a)

Simply supported (S):

$U = W_b = W_s$

$$= B_{11}\frac{\partial U}{\partial x} - \left(D_{11} + A_m\right)\frac{\partial^2 W_b}{\partial x^2} - \left[D_{11}^s + \frac{1}{2}\left(A_m + B_m\right)\right]\frac{\partial^2 W_s}{\partial x^2} + L_{13}W_z - \frac{1}{2}E_m\frac{\partial^2 W_z}{\partial x^2}$$

$$= B_{11}^s\frac{\partial U}{\partial x} - \left[D_{11}^s + \frac{1}{2}\left(A_m + B_m\right)\right]\frac{\partial^2 W_b}{\partial x^2} - \left[H_{11} + \frac{1}{4}\left(A_m + 2B_m + C_m\right)\right]\frac{\partial^2 W_s}{\partial x^2} + L_{13}^s W_z - \frac{1}{4}\left(E_m + D_m\right)\frac{\partial^2 W_z}{\partial x^2}$$

$$= E_m\frac{\partial^2 W_b}{\partial x^2} + \frac{1}{2}\left(E_m + D_m\right)\frac{\partial^2 W_s}{\partial x^2} + \frac{1}{2}F_m\frac{\partial^2 W_z}{\partial x^2} = 0 \quad (25b)$$

Free (F):

$$A_{11}\frac{\partial U}{\partial x} - B_{11}\frac{\partial^2 W_b}{\partial x^2} - B_{11}^s\frac{\partial^2 W_s}{\partial x^2} + K_{13}W_z$$

$$= B_{11}a_1 U + B_{11}\left(\frac{n_x}{a} + a_2\right)\frac{\partial U}{\partial x}$$

$$+\left(B_{11}a_3 - I_2\omega^2\right)\frac{\partial W_b}{\partial x} + \left[\left(B_{11}a_4 - \frac{n_x}{a}\right)D_{11} - \frac{n_x}{a}A_m\right]\frac{\partial^2 W_b}{\partial x^2} + \left[\left(B_{11}a_5 - D_{11}\right) - A_m\right]\frac{\partial^3 W_b}{\partial x^3}$$

$$+\left(B_{11}a_6 - J_2\omega^2\right)\frac{\partial W_s}{\partial x} + \left[\left(B_{11}a_7 - \frac{n_x}{a}D_{11}^s\right) - \frac{1}{2}\frac{n_x}{a}\left(A_m + B_m\right)\right]\frac{\partial^2 W_s}{\partial x^2} + \left[\left(B_{11}a_8 - D_{11}^s\right) - \frac{1}{2}\left(A_m + B_m\right)\right]\frac{\partial^3 W_s}{\partial x^3}$$

$$+\left(B_{11}a_9 + \frac{n_x}{a}L_{13}\right)W_z + \left(B_{11}a_{10} + L_{13}\right)\frac{\partial W_z}{\partial x} - \frac{1}{2}\frac{n_x}{a}E_m\frac{\partial^2 W_z}{\partial x^2} - \frac{1}{2}E_m\frac{\partial^3 W_z}{\partial x^3}$$

$$= B_{11}\frac{\partial U}{\partial x} - \left(D_{11} + A_m\right)\frac{\partial^2 W_b}{\partial x^2} - \left[D_{11}^s + \frac{1}{2}\left(A_m + B_m\right)\right]\frac{\partial^2 W_s}{\partial x^2} + L_{13}W_z - \frac{1}{2}E_m\frac{\partial^2 W_z}{\partial x^2}$$

$$= J_1\omega^2 U + B_{11}^s\frac{\partial U}{\partial x} - J_2\omega^2\frac{\partial W_b}{\partial x} - \left(D_{11}^s + \frac{1}{2}\frac{n_x}{a}\left(A_m + B_m\right)\right)\frac{\partial^2 W_b}{\partial x^2} - \frac{1}{2}\left(A_m + B_m\right)\frac{\partial^3 W_b}{\partial x^3}$$

$$+\left(A_{55}^s + \frac{1}{4}H_m - K_2\omega^2\right)\frac{\partial W_s}{\partial x} - \left[H_{11} + \frac{1}{4}\frac{n_x}{a}\left(A_m + 2B_m + C_m\right)\right]\frac{\partial^2 W_s}{\partial x^2} - \frac{1}{4}\left(A_m + 2B_m + C_m\right)\frac{\partial^3 W_s}{\partial x^3}$$

$$+L_{13}^s W_z + \left(A_{55}^s - \frac{1}{4}H_m\right)\frac{\partial W_z}{\partial x} - \frac{1}{4}\frac{n_x}{a}\left(E_m + D_m\right)\frac{\partial^2 W_z}{\partial x^2} - \frac{1}{4}\left(E_m + D_m\right)\frac{\partial^3 W_z}{\partial x^3}$$

$$= B_{11}^s\frac{\partial U}{\partial x} - \left[D_{11}^s + \frac{1}{2}\left(A_m + B_m\right)\right]\frac{\partial^2 W_b}{\partial x^2} - \left[H_{11} + \frac{1}{4}\left(A_m + 2B_m + C_m\right)\right]\frac{\partial^2 W_s}{\partial x^2} + L_{13}^s W_z - \frac{1}{4}\left(E_m + D_m\right)\frac{\partial^2 W_z}{\partial x^2}$$

$$= -\frac{1}{2}\frac{n_x}{a}E_m\frac{\partial^2 W_b}{\partial x^2} - \frac{1}{2}E_m\frac{\partial^3 W_b}{\partial x^3} + \left(A_{55}^s + \frac{1}{4}H_m\right)\frac{\partial W_s}{\partial x} - \frac{1}{4}\frac{n_x}{a}\left(E_m + D_m\right)\frac{\partial^2 W_s}{\partial x^2} - \frac{1}{4}\left(E_m + D_m\right)\frac{\partial^3 W_s}{\partial x^3}$$

$$+\left(A_{55}^s - \frac{1}{4}H_m\right)\frac{\partial W_z}{\partial x} - \frac{1}{4}\frac{n_x}{a}F_m\frac{\partial^2 W_z}{\partial x^2} - \frac{1}{4}F_m\frac{\partial^3 W_z}{\partial x^3}$$

$$= E_m\frac{\partial^2 W_b}{\partial x^2} + \frac{1}{2}\left(E_m + D_m\right)\frac{\partial^2 W_s}{\partial x^2} + \frac{1}{2}F_m\frac{\partial^2 W_z}{\partial x^2} = 0 \tag{25c}$$

By substituting Eq. (23) into Eq. (25) with the required BCs, a system of equations is obtained as:

$$\boldsymbol{\alpha}\mathbf{e}^{\mathbf{Tx}}\mathbf{K} = \mathbf{0} \tag{26}$$

where $\boldsymbol{\alpha}$ comes from the coefficients in Eq. (25) for the appropriate BCs at $x = \pm a/2$. The natural frequencies ω_n of the nth mode of vibration can be obtained by setting $\left|\boldsymbol{\alpha}\mathbf{e}^{\mathbf{Tx}}\right| = 0$. It is noticeable that the iteration procedure [71] is used in this paper to calculate the natural frequencies. The mode shapes are plotted by solving for $\mathbf{K}$ from Eq. (26) based on the singular value decomposition, and calculating the displacement components along the beams thereafter.

4. Numerical results and discussion

In this session, the numerical examples are presented to investigate the size-dependent vibration behaviours of conventional FG and BDFG microbeams using the HOBT and quasi-3D theory. In the first part, the natural frequencies of conventional FG microbeams (Type A) under arbitrary BCs are analysed. The beams are made of SiC $\left(E_c = 427GPa, \rho_c = 3100\,kg/m^3, \upsilon_c = 0.17\right)$ and Al $\left(E_m = 70GPa, \rho_m = 2702\,kg/m^3, \upsilon_m = 0.3\right)$. The non-dimensional natural frequencies are defined as follows: $\bar{\Omega} = \frac{\omega a^2}{h}\sqrt{\frac{\rho_m}{E_m}}$ and $\tilde{\Omega} = \frac{\omega a}{h}\sqrt{\frac{I_{10}}{A_{110}}}$ with $I_{10} = \int_{-h/2}^{h/2}\frac{E_m}{1-\upsilon_m^2}$ and $A_{110} = \int_{-h/2}^{h/2}\rho_m$. The second part deals with the free vibration response of BDFG microbeams (Types B and C). The base material properties in BDFG microbeams are $E_0 = 210GPa, \rho_0 = 7850\,kg/m^3$ and $\upsilon_0 = 0.3$. The following non-dimensional natural frequency $\hat{\Omega} = \frac{\omega a^2}{h}\sqrt{\frac{\rho_0}{E_0}}$ is used. Since the BDFG beams are not horizontally symmetric as discussed later, it is useful to clarify that the two letters, e.g. C-S, are used to describe the BCs at the left and right ends of the beam, respectively.

4.1. Conventional FG microbeams

The natural frequencies of SiC/Al microbeams under various thickness-to-material length scale ratios are given in Table 1. The obtained solutions for the C-C and S-S microbeams agree well with those based on the FOBT [12] and HOBT [72]. The effect of BCs on the natural frequencies is also highlighted in this table. It can be seen that the highest frequencies are seen in C-C beams and followed by C-S, F-S, S-S and C-F beams as expected. It is worth noting that the Poisson effect is included in both thickness and longitudinal directions, and the Mori-Tanaka scheme is used in this table. The corresponding formula can be found in [12, 32, 42]. Further to the C-C microbeams, the difference between the vibration mode shapes predicted by the HOBT and quasi-3D theory is revealed in Fig. 2 for the first three modes. It can be seen that the stretching effect is more noticeable for the thick beams and the higher modes. In addition, the axial mode appears in the second mode instead of the third mode as in the case of macrobeams as observed in Ref. [73].

Table 2 and Fig. 3 examine the effect of the power-law index and the BCs in both FG micro- and macro-beams. As expected, the natural frequencies gradually decrease with a reduction of ceramic volume fraction, which results in a lower Young's modulus. For simply supported beams, unlike the Navier solution [42], the present approach can be employed to adapt the requirements of both displacement and stress resultants. Therefore, it is applicable to both immovable (S_1) and movable (S_2) simply supported BCs. Using these two BCs (S_1-S_1 and S_1-S_2), the difference between the natural frequencies and the first three mode shapes for microbeams $\left(n_z = 2\right)$ is shown in Table 2 and Fig. 4. These two BCs only result in the identical frequencies for the homogeneous beam $\left(n_z = 0\right)$ as expected, whereas the S_1-S_1 BC leads to the higher values for the FG beams. The difference is more apparent in the higher modes, where the axial modes appear in the movable simply supported beams with quite low frequencies. In the rest of this paper, the movable simply support is combined with other end conditions, except for the free end that joins with the immovable one. The simply supported beams are assembled by an immovable support at $x = -a/2$ and a movable one at $x = a/2$. Comparing various BCs, the higher frequencies are observed in the beams with stiffer ends, i.e. C-C, and with a higher volume of ceramic (smaller n_z). It is interesting

that the fundamental frequencies of the S-F beams are nearly the same with those of C-S beams for both micro and macroscales.

The difference between the vibration behaviour of macro and microbeams is also seen in the mode shapes. Fig. 5 demonstrates the variation of the vibration mode shapes with respect to the change of the frequencies. These graphs can be used to state the mode shapes where the change of the number of half-sine waves occurs. As can be seen from this figure, for C-C and F-C beams, there is a significant change between the vibration mode shapes in the macrobeams. However, in the microbeams, they are not too prominent to the neighbour status.

4.2. BDFG beams

Tables 3-6 reveal the fundamental frequencies of BDFG beams (Types B and C) with respect to different BCs, exponential indices and thickness-to-material length scales. The current results for macrobeams ($h/l=\infty$) agree well with those given by Simsek [58]. The natural frequencies of Types B and C are identical for the conventional FG beam $\left(n_z=0\right)$, but they are different for BDFG beams. The lower frequencies are observed with the elevated n_z, but the change is more significant from the symmetric cross-section beams, i.e. Type C. This correlation is also presented in Fig. 6, which illustrates the effect of axial and through-the-thickness exponential indices to the natural frequencies of BDFG microbeams under various BCs. It is seen that the increase of n_z leads to a reduction in frequencies in all cases, whereas the increase of n_x only leads to a reduction in frequencies of C-S, S-S and C-F beams. In order to illustrate solely the effect of material properties in each direction, Fig. 7 plots the relationship between the natural frequencies and thickness-to-material length scales for the axial and through-the-thickness FG beams. In both cases, the effect of couple stress is negligible as the thickness is greater than $30l$. For the conventional FG beams, the natural frequencies are lower in Type C, while they are identical in the axial FG beams as expected.

As mentioned before that the BDFG beams are not horizontally symmetric which means that the switching of the left and right BCs, e.g. C-F and F-C, changes the natural frequencies and vibration mode shapes. An example of switching C-F and C-S BCs is demonstrated in Fig. 8. In both cases, the left

clamped ends cause lower frequency with the elevated n_x, which is opposite to the right clamped ends do. Indeed, the increase of n_x results in an increase of not only Young's modulus but also the density. When the clamps are placed at the stiffer and heavier ends (the right ends), the natural frequencies are maximised. Finally, the effect of n_x in the mode shapes of several BCs is revealed in Fig. 9 with n_z equal to 2. For the C-C beams, the mode shapes are not symmetric for non-zero n_x, where the maximum modal displacement is seen on the left half. For the F-C beams, in which the maximum displacement occurs at the tip, the small relative magitudes are seen on other points. In addition, the second mode is the flexural mode for through-the-thickness FG beams $\left(n_x = 0\right)$; however, the axial one for BDFG beams $\left(n_x \neq 0\right)$.

5. Conclusions

In this paper, state-space based solutions are presented for the free vibration behaviour of conventional and BDFG microbeams under arbitrary boundary conditions. Based on the Hamilton's principle and the modified couple stress theory, the governing equations of motion are developed for the quasi-3D theory. The natural frequencies are obtained via an iteration procedure and the corresponding mode shapes are outlined by the singular value decomposition. It is concluded that both the natural frequencies and mode shapes are significantly different between macro and microbeams, emphasizing the need of employing the non-classical continua for small-scale structures. The inclusion of the size effect results in a considerable increase in the bending stiffness and the switching between flexural and axial modes. It is also worth noting that due to the asymmetric along the length, the employing of BCs in analysing the BDFG beams needs to perform with the clarification of the left and right ends.

References

[1] Yang F, Chong ACM, Lam DCC, Tong P. Couple stress based strain gradient theory for elasticity. International Journal of Solids and Structures. 2002;39:2731–43

[2] Toupin RA. Elastic materials with couple stresses. Archives of Rational of Mechanical and Analysis. 1962;11:385–414

[3] Mindlin RD, Tiersten HF. Effects of couple-stresses in linear elasticity. Archives of Rational Mechanics and Analysis. 1962;11:415–48

[4] Koiter WT. Couple stresses in the theory of elasticity. I and II Proc K Ned Akad Wet 1964;B(67):17-44

[5] Mindlin RD. Micro-structure in linear elasticity. Archives of Rational Mechanics and Analysis. 1964;16:51-78

[6] Park SK, Gao XL. Bernoulli–Euler beam model based on a modified couple stress theory. Journal of Micromechanics and Microengineering. 2006;16(11):2355-9

[7] Kong S, Zhou S, Nie Z, Wang K. The size-dependent natural frequency of Bernoulli–Euler micro-beams. International Journal of Engineering Science. 2008;46(5):427-37

[8] Xia W, Wang L, Yin L. Nonlinear non-classical microscale beams: Static bending, postbuckling and free vibration. International Journal of Engineering Science. 2010;48(12):2044-53

[9] Ma H, Gao X, Reddy J. A microstructure-dependent Timoshenko beam model based on a modified couple stress theory. Journal of the Mechanics and Physics of Solids. 2008;56(12):3379-91

[10] Asghari M, Ahmadian MT, Kahrobaiyan MH, Rahaeifard M. On the size-dependent behavior of functionally graded micro-beams. Materials & Design. 2010;31(5):2324-9

[11] Ke L-L, Wang Y-S. Size effect on dynamic stability of functionally graded microbeams based on a modified couple stress theory. Composite Structures. 2011;93(2):342-50

[12] Ke L-L, Wang Y-S, Yang J, Kitipornchai S. Nonlinear free vibration of size-dependent functionally graded microbeams. International Journal of Engineering Science. 2012;50(1):256-67

[13] Dehrouyeh-Semnani AM, Mostafaei H, Nikkhah-Bahrami M. Free flexural vibration of geometrically imperfect functionally graded microbeams. International Journal of Engineering Science. 2016;105:56-79

[14] Reddy JN. Microstructure-dependent couple stress theories of functionally graded beams. Journal of the Mechanics and Physics of Solids. 2011;59(11):2382-99

[15] Şimşek M, Kocatürk T, Akbaş ŞD. Static bending of a functionally graded microscale Timoshenko beam based on the modified couple stress theory. Composite Structures. 2013;95:740-7

[16] Kahrobaiyan MH, Asghari M, Ahmadian MT. A Timoshenko beam element based on the modified couple stress theory. International Journal of Mechanical Sciences. 2014;79:75-83

[17] Thai H-T, Vo TP, Nguyen T-K, Lee J. Size-dependent behavior of functionally graded sandwich microbeams based on the modified couple stress theory. Composite Structures. 2015;123:337-49

[18] Nateghi A, Salamat-talab M. Thermal effect on size dependent behavior of functionally graded microbeams based on modified couple stress theory. Composite Structures. 2013;96:97-110

[19] Akgöz B, Civalek Ö. Free vibration analysis of axially functionally graded tapered Bernoulli–Euler microbeams based on the modified couple stress theory. Composite Structures. 2013;98:314-22

[20] Filippi M, Carrera E. Bending and vibrations analyses of laminated beams by using a zig-zag-layer-wise theory. Composites Part B: Engineering. 2016;98:269-80

[21] Frikha A, Hajlaoui A, Wali M, Dammak F. A new higher order C0 mixed beam element for FGM beams analysis. Composites Part B: Engineering. 2016;106:181-9

[22] Giunta G, De Pietro G, Nasser H, Belouettar S, Carrera E, Petrolo M. A thermal stress finite element analysis of beam structures by hierarchical modelling. Composites Part B: Engineering. 2016;95:179-95

[23] Gupta A, Talha M, Singh BN. Vibration characteristics of functionally graded material plate with various boundary constraints using higher order shear deformation theory. Composites Part B: Engineering. 2016;94:64-74

[24] Li D, Deng Z, Xiao H. Thermomechanical bending analysis of functionally graded sandwich plates using four-variable refined plate theory. Composites Part B: Engineering. 2016;106:107-19

[25] Mantari JL, Canales FG. Finite element formulation of laminated beams with capability to model the thickness expansion. Composites Part B: Engineering. 2016;101:107-15

[26] Nguyen T-K, Nguyen V-H, Chau-Dinh T, Vo TP, Nguyen-Xuan H. Static and vibration analysis of isotropic and functionally graded sandwich plates using an edge-based MITC3 finite elements. Composites Part B: Engineering. 2016;107:162-73

[27] Hui Y, Giunta G, Belouettar S, Huang Q, Hu H, Carrera E. A free vibration analysis of three-dimensional sandwich beams using hierarchical one-dimensional finite elements. Composites Part B: Engineering. 2017;110:7-19

[28] Mechab I, El Meiche N, Bernard F. Analytical study for the development of a new warping function for high order beam theory. Composites Part B: Engineering. 2017;119:18-31

[29] Shao D, Hu S, Wang Q, Pang F. Free vibration of refined higher-order shear deformation composite laminated beams with general boundary conditions. Composites Part B: Engineering. 2017;108:75-90

[30] Nateghi A, Salamat-talab M, Rezapour J, Daneshian B. Size dependent buckling analysis of functionally graded micro beams based on modified couple stress theory. Applied Mathematical Modelling. 2012;36(10):4971-87

[31] Salamat-talab M, Nateghi A, Torabi J. Static and dynamic analysis of third-order shear deformation FG micro beam based on modified couple stress theory. International Journal of Mechanical Sciences. 2012;57(1):63-73

[32] Ansari R, Gholami R, Faghih Shojaei M, Mohammadi V, Sahmani S. Size-dependent bending, buckling and free vibration of functionally graded Timoshenko microbeams based on the most general strain gradient theory. Composite Structures. 2013;100:385-97

[33] Sahmani S, Ansari R. Size-dependent buckling analysis of functionally graded third-order shear deformable microbeams including thermal environment effect. Applied Mathematical Modelling. 2013;37(23):9499-515

[34] Mohammad-Abadi M, Daneshmehr AR. Size dependent buckling analysis of microbeams based on modified couple stress theory with high order theories and general boundary conditions. International Journal of Engineering Science. 2014;74:1-14

[35] Şimşek M, Reddy JN. Bending and vibration of functionally graded microbeams using a new higher order beam theory and the modified couple stress theory. International Journal of Engineering Science. 2013;64:37-53

[36] Akgöz B, Civalek Ö. Thermo-mechanical buckling behavior of functionally graded microbeams embedded in elastic medium. International Journal of Engineering Science. 2014;85:90-104

[37] Akgöz B, Civalek Ö. Shear deformation beam models for functionally graded microbeams with new shear correction factors. Composite Structures. 2014;112:214-25

[38] Darijani H, Mohammadabadi H. A new deformation beam theory for static and dynamic analysis of microbeams. International Journal of Mechanical Sciences. 2014;89:31-9

[39] Al-Basyouni KS, Tounsi A, Mahmoud SR. Size dependent bending and vibration analysis of functionally graded micro beams based on modified couple stress theory and neutral surface position. Composite Structures. 2015;125:621-30

[40] Arbind A, Reddy JN. Nonlinear analysis of functionally graded microstructure-dependent beams. Composite Structures. 2013;98:272-81

[41] Arbind A, Reddy JN, Srinivasa AR. Modified Couple Stress-Based Third-Order Theory for Nonlinear Analysis of Functionally Graded Beams. Latin American journal of solids and structures. 2014;11:459-87

[42] Trinh LC, Nguyen HX, Vo TP, Nguyen T-K. Size-dependent behaviour of functionally graded microbeams using various shear deformation theories based on the modified couple stress theory. Composite Structures. 2016;154:556-72

[43] Eringen AC. On differential equations of nonlocal elasticity and solutions of screw dislocation and surface waves. Journal of Applied Physics. 1983;54:4703-10

[44] Romanoff J, Reddy JN, Jelovica J. Using non-local Timoshenko beam theories for prediction of micro- and macro-structural responses. Composite Structures. 2016;156:410-20

[45] Reddy JN, El-Borgi S, Romanoff J. Non-linear analysis of functionally graded microbeams using Eringen′s non-local differential model. International Journal of Non-Linear Mechanics. 2014;67:308-18

[46] Apuzzo A, Barretta R, Canadija M, Feo L, Luciano R, Marotti de Sciarra F. A closed-form model for torsion of nanobeams with an enhanced nonlocal formulation. Composites Part B: Engineering. 2017;108:315-24

[47] Romano G, Barretta R. Stress-driven versus strain-driven nonlocal integral model for elastic nano-beams. Composites Part B: Engineering. 2017;114:184-8

[48] Romano G, Barretta R, Diaco M. Micromorphic continua: non-redundant formulations. Continuum Mechanics and Thermodynamics. 2016;28(6):1659-70

[49] Barretta R, Feo L, Luciano R, Marotti de Sciarra F. Application of an enhanced version of the Eringen differential model to nanotechnology. Composites Part B: Engineering. 2016;96:274-80

[50] Barretta R, Feo L, Luciano R, Marotti de Sciarra F, Penna R. Functionally graded Timoshenko nanobeams: A novel nonlocal gradient formulation. Composites Part B: Engineering. 2016;100:208-19

[51] Barretta R, Feo L, Luciano R, Marotti de Sciarra F. An Eringen-like model for Timoshenko nanobeams. Composite Structures. 2016;139:104-10

[52] Mindlin RD. Second gradient of strain and surface tension in linear elasticity. Archive for Rational Mechanics and Analysis. 1965;16:51-78

[53] Fleck NA, Hutchinson JW. A reformulation of strain gradient plasticity. Journal of the Mechanics and Physics of Solids. 2001;49:2245-71

[54] Lam DCC, Yang F, Chong ACM, Wang J, Tong P. Experiments and theory in strain gradient elasticity. Journal of the Mechanics and Physics of Solids. 2003;51(8):1477-508

[55] Thai H-T, Vo TP, Nguyen T-K, Kim S-E. A review of continuum mechanics models for size-dependent analysis of beams and plates. Composite Structures. 2017;177:196-219

[56] Lü CF, Chen WQ, Xu RQ, Lim CW. Semi-analytical elasticity solutions for bi-directional functionally graded beams. International Journal of Solids and Structures. 2008;45(1):258-75

[57] Lezgy-Nazargah M. Fully coupled thermo-mechanical analysis of bi-directional FGM beams using NURBS isogeometric finite element approach. Aerospace Science and Technology. 2015;45:154-64

[58] Şimşek M. Bi-directional functionally graded materials (BDFGMs) for free and forced vibration of Timoshenko beams with various boundary conditions. Composite Structures. 2015;133:968-78

[59] Şimşek M. Buckling of Timoshenko beams composed of two-dimensional functionally graded material (2D-FGM) having different boundary conditions. Composite Structures. 2016;149:304-14

[60] Hao D, Wei C. Dynamic characteristics analysis of bi-directional functionally graded Timoshenko beams. Composite Structures. 2016;141:253-63

[61] Huynh TA, Lieu XQ, Lee J. NURBS-based modeling of bidirectional functionally graded Timoshenko beams for free vibration problem. Composite Structures. 2017;160:1178-90

[62] Karamanlı A. Elastostatic analysis of two-directional functionally graded beams using various beam theories and Symmetric Smoothed Particle Hydrodynamics method. Composite Structures. 2017;160:653-69

[63] Karamanlı A. Bending behaviour of two directional functionally graded sandwich beams by using a quasi-3d shear deformation theory. Composite Structures. 2017;174:70-86

[64] Nejad MZ, Hadi A. Eringen's non-local elasticity theory for bending analysis of bi-directional functionally graded Euler–Bernoulli nano-beams. International Journal of Engineering Science. 2016;106:1-9

[65] Nejad MZ, Hadi A. Non-local analysis of free vibration of bi-directional functionally graded Euler–Bernoulli nano-beams. International Journal of Engineering Science. 2016;105:1-11

[66] Nejad MZ, Hadi A, Rastgoo A. Buckling analysis of arbitrary two-directional functionally graded Euler–Bernoulli nano-beams based on nonlocal elasticity theory. International Journal of Engineering Science. 2016;103:1-10

[67] Shafiei N, Kazemi M. Buckling analysis on the bi-dimensional functionally graded porous tapered nano-/micro-scale beams. Aerospace Science and Technology. 2017;66:1-11

[68] Shafiei N, Mirjavadi SS, MohaselAfshari B, Rabby S, Kazemi M. Vibration of two-dimensional imperfect functionally graded (2D-FG) porous nano-/micro-beams. Computer Methods in Applied Mechanics and Engineering. 2017;322:615-32

[69] Vo TP, Thai H-T, Nguyen T-K, Lanc D, Karamanli A. Flexural analysis of laminated composite and sandwich beams using a four-unknown shear and normal deformation theory. Composite Structures. 2017;176:388-97

[70] Vo TP, Thai H-T, Aydogdu M. Free vibration of axially loaded composite beams using a four-unknown shear and normal deformation theory. Composite Structures. 2017;178:406-14

[71] Thai HT, Kim SE. Levy-type solution for free vibration analysis of orthotropic plates based on two variable refined plate theory. Applied Mathematical Modelling. 2012;36(8):3870-82

[72] Ansari R, Shojaei MF, Gholami R. Size-dependent nonlinear mechanical behavior of third-order shear deformable functionally graded microbeams using the variational differential quadrature method. Composite Structures. 2016;136:669-83

[73] Trinh LC, Vo TP, Thai H-T, Nguyen T-K. An analytical method for the vibration and buckling of functionally graded beams under mechanical and thermal loads. Composites Part B: Engineering. 2016;100:152-63

Appendix

The coefficients in Eq. (19):

$$a_1=\frac{-I_0\omega^2}{A_{11}};a_2=\frac{-\frac{n_x}{a}A_{11}}{A_{11}};a_3=\frac{I_1\omega^2}{A_{11}};a_4=\frac{\frac{n_x}{a}B_{11}}{A_{11}};a_5=\frac{B_{11}}{A_{11}};$$

$$a_6=\frac{J_1\omega^2}{A_{11}};a_7=\frac{\frac{n_x}{a}B_{11}^s}{A_{11}};a_8=\frac{B_{11}^s}{A_{11}};a_9=\frac{-\frac{n_x}{a}K_{13}}{A_{11}};a_{10}=\frac{-K_{13}}{A_{11}}. \tag{A1}$$

$$r_1=\left[c_3f_2e_4-e_3f_2c_4+f_3\left(e_2c_4-c_2e_4\right)\right]/C_0;$$

$$r_2=\left[c_3\left(f_2e_5-e_2f_4\right)-e_3\left(f_2c_5-c_2f_4\right)+f_3\left(e_2c_5-c_2e_5\right)\right]/C_0;$$

$$r_3=\left[c_3\left(f_2e_6-e_2f_5\right)-e_3\left(f_2c_6-c_2f_5\right)+f_3\left(e_2c_6-c_2e_6\right)\right]/C_0;$$

$$r_4=\left[c_3f_2e_7-e_3f_2c_7+f_3\left(e_2c_7-c_2e_7\right)\right];$$

$$r_5=\left[c_3\left(f_2e_8-e_2f_6\right)-e_3\left(f_2c_8-c_2f_6\right)+f_3\left(e_2c_8-c_2e_8\right)\right]/C_0;$$

$$r_6=\left[c_3\left(f_2e_9-e_2f_7\right)-e_3\left(f_2c_9-c_2f_7\right)+f_3\left(e_2c_9-c_2e_9\right)\right]/C_0;$$

$$r_7=\left[c_3\left(f_2e_{10}-e_2f_8\right)-e_3\left(f_2c_{10}-c_2f_8\right)+f_3\left(e_2c_{10}-c_2e_{10}\right)\right]/C_0;$$

$$r_8=\left[c_3\left(f_2e_{11}-e_2f_9\right)-e_3\left(f_2c_{11}-c_2f_9\right)+f_3\left(e_2c_{11}-c_2e_{11}\right)\right]/C_0;$$

$$r_9=\left[c_3\left(f_2e_{12}-e_2f_{10}\right)-e_3\left(f_2c_{12}-c_2f_{10}\right)+f_3\left(e_2c_{12}-c_2e_{12}\right)\right]/C_0;$$

$$r_{10}=\left[c_3\left(f_2e_{13}-e_2f_{11}\right)-e_3\left(f_2c_{13}-c_2f_{11}\right)+f_3\left(e_2c_{13}-c_2e_{13}\right)\right]/C_0;$$

$$r_{11}=\left[c_3\left(f_2e_{14}-e_2f_{12}\right)-e_3\left(f_2c_{14}-c_2f_{12}\right)+f_3\left(e_2c_{14}-c_2e_{14}\right)\right]/C_0;$$

$$r_{12}=\left[c_3\left(f_2e_{15}-e_2f_{13}\right)-e_3\left(f_2c_{15}-c_2f_{13}\right)+f_3\left(e_2c_{15}-c_2e_{15}\right)\right]/C_0;$$

$$r_{13}=c_3\left(f_2e_{16}-e_2f_{14}\right)-e_3\left(f_2c_{16}-c_2f_{14}\right)+f_3\left(e_2c_{16}-c_2e_{16}\right)/C_0;$$

$$r_{14}=\left[c_3\left(f_2e_{17}-e_2f_{15}\right)-e_3\left(f_2c_{17}-c_2f_{15}\right)+f_3\left(e_2c_{17}-c_2e_{17}\right)\right]/C_0. \tag{A2}$$

$$s_1=\left[c_1f_3e_4-e_1f_3c_4+f_1\left(e_3c_4-c_3e_4\right)\right]/C_0;$$

$$s_2=\left[c_1\left(f_3e_5-e_3f_4\right)-e_1\left(f_3c_5-c_3f_4\right)+f_1\left(e_3c_5-c_3e_5\right)\right]/C_0;$$

$$s_3=\left[c_1\left(f_3e_6-e_3f_5\right)-e_1\left(f_3c_6-c_3f_5\right)+f_1\left(e_3c_6-c_3e_6\right)\right]/C_0;$$

$$s_4=\left[c_1f_3e_7-e_1f_3c_7+f_1\left(e_3c_7-c_3e_7\right)\right]/C_0;$$

$$s_5=\left[c_1\left(f_3e_8-e_3f_6\right)-e_1\left(f_3c_8-c_3f_6\right)+f_1\left(e_3c_8-c_3e_8\right)\right]/C_0;$$

$$s_6=\left[c_1\left(f_3e_9-e_3f_7\right)-e_1\left(f_3c_9-c_3f_7\right)+f_1\left(e_3c_9-c_3e_9\right)\right]/C_0;$$

$$s_7=\left[c_1\left(f_3e_{10}-e_3f_8\right)-e_1\left(f_3c_{10}-c_3f_8\right)+f_1\left(e_3c_{10}-c_3e_{10}\right)\right]/C_0;$$

$$s_8=\left[c_1\left(f_3e_{11}-e_3f_9\right)-e_1\left(f_3c_{11}-c_3f_9\right)+f_1\left(e_3c_{11}-c_3e_{11}\right)\right]/C_0;$$

$$s_9=\left[c_1\left(f_3e_{12}-e_3f_{10}\right)-e_1\left(f_3c_{12}-c_3f_{10}\right)+f_1\left(e_3c_{12}-c_3e_{12}\right)\right]/C_0;$$

$$s_{10}=\left[c_1\left(f_3e_{13}-e_3f_{11}\right)-e_1\left(f_3c_{13}-c_3f_{11}\right)+f_1\left(e_3c_{13}-c_3e_{13}\right)\right]/C_0;$$

$$s_{11}=\left[c_1\left(f_3e_{14}-e_3f_{12}\right)-e_1\left(f_3c_{14}-c_3f_{12}\right)+f_1\left(e_3c_{14}-c_3e_{14}\right)\right]/C_0;$$

$$s_{12}=\left[c_1\left(f_3e_{15}-e_3f_{13}\right)-e_1\left(f_3c_{15}-c_3f_{13}\right)+f_1\left(e_3c_{15}-c_3e_{15}\right)\right]/C_0;$$

$$s_{13}=\left[c_1\left(f_3e_{16}-e_3f_{14}\right)-e_1\left(f_3c_{16}-c_3f_{14}\right)+f_1\left(e_3c_{16}-c_3e_{16}\right)\right]/C_0;$$

$$s_{14}=\left[c_1\left(f_3e_{17}-e_3f_{15}\right)-e_1\left(f_3c_{17}-c_3f_{15}\right)+f_1\left(e_3c_{17}-c_3e_{17}\right)\right]/C_0. \tag{A3}$$

$$t_1=\left[-c_1f_2e_4+e_1f_2c_4+f_1\left(c_2e_4-e_2c_4\right)\right]/C_0;$$

$$t_2=\left[c_1\left(e_2f_4-f_2e_5\right)-e_1\left(c_2f_4-f_2c_5\right)+f_1\left(c_2e_5-e_2c_5\right)\right]/C_0;$$

$$t_3=\left[c_1\left(e_2f_5-f_2e_6\right)-e_1\left(c_2f_5-f_2c_6\right)+f_1\left(c_2e_6-e_2c_6\right)\right];$$

$$t_4=\left[-c_1f_2e_7+e_1f_2c_7+f_1\left(c_2e_7-e_2c_7\right)\right]/C_0;$$

$$t_5=\left[c_1\left(e_2f_6-f_2e_8\right)-e_1\left(c_2f_6-f_2c_8\right)+f_1\left(c_2e_8-e_2c_8\right)\right]/C_0;$$

$$t_6=\left[c_1\left(e_2f_7-f_2e_9\right)-e_1\left(c_2f_7-f_2c_9\right)+f_1\left(c_2e_9-e_2c_9\right)\right]/C_0;$$

$$t_7=\left[c_1\left(e_2f_8-f_2e_{10}\right)-e_1\left(c_2f_8-f_2c_{10}\right)+f_1\left(c_2e_{10}-e_2c_{10}\right)\right]/C_0;$$

$$t_8=\left[c_1\left(e_2f_9-f_2e_{11}\right)-e_1\left(c_2f_9-f_2c_{11}\right)+f_1\left(c_2e_{11}-e_2c_{11}\right)\right]/C_0;$$

$$t_9=\left[c_1\left(e_2f_{10}-f_2e_{12}\right)-e_1\left(c_2f_{10}-f_2c_{12}\right)+f_1\left(c_2e_{12}-e_2c_{12}\right)\right]/C_0;$$

$$t_{10}=\left[c_1\left(e_2f_{11}-f_2e_{13}\right)-e_1\left(c_2f_{11}-f_2c_{13}\right)+f_1\left(c_2e_{13}-e_2c_{13}\right)\right]/C_0;$$

$$t_{11}=\left[c_1\left(e_2f_{12}-f_2e_{14}\right)-e_1\left(c_2f_{12}-f_2c_{14}\right)+f_1\left(c_2e_{14}-e_2c_{14}\right)\right]/C_0;$$

$$t_{12}=\left[c_1\left(e_2f_{13}-f_2e_{15}\right)-e_1\left(c_2f_{13}-f_2c_{15}\right)+f_1\left(c_2e_{15}-e_2c_{15}\right)\right]/C_0;$$

$$t_{13}=\left[c_1\left(e_2f_{14}-f_2e_{16}\right)-e_1\left(c_2f_{14}-f_2c_{16}\right)+f_1\left(c_2e_{16}-e_2c_{16}\right)\right]/C_0;$$

$$t_{14}=\left[c_1\left(e_2f_{15}-f_2e_{17}\right)-e_1\left(c_2f_{15}-f_2c_{17}\right)+f_1\left(c_2e_{17}-e_2c_{17}\right)\right]/C_0. \tag{A4}$$

where $C_0=c_1\left(e_2f_3-e_3f_2\right)-c_2\left(e_1f_3-e_3f_1\right)+c_3\left(e_1f_2-e_2f_1\right)$.

$$b_1 = D_{11} + A_m; b_2 = D_{11}^s + \frac{1}{2}\left(A_m + B_m\right); b_3 = \frac{1}{2}E_m; b_4 = \frac{n_x}{a}I_1\omega^2; b_5 = \left(\frac{n_x}{a}\right)^2 B_{11} + I_1\omega^2; b_6 = 2\frac{n_x}{a}B_{11};$$

$$b_7 = B_{11}; b_8 = I_0\omega^2; b_9 = -\frac{n_x}{a}I_2\omega^2; b_{10} = -\left(\frac{n_x}{a}\right)^2\left(D_{11} + A_m\right) - I_2\omega^2; b_{11} = -2\frac{n_x}{a}\left(D_{11} + A_m\right);$$

$$b_{12} = I_0\omega^2; b_{13} = -\frac{n_x}{a}J_2\omega^2; b_{14} = -\left(\frac{n_x}{a}\right)^2\left[D_{11}^s + \frac{1}{2}\left(A_m + B_m\right)\right] - J_2\omega^2; b_{15} = -\frac{n_x}{a}\left[2D_{11}^s + \left(A_m + B_m\right)\right];$$

$$b_{16} = \left(\frac{n_x}{a}\right)^2 L_{13} + J_0\omega^2; b_{17} = 2\frac{n_x}{a}L_{13}; b_{18} = L_{13} - \frac{1}{2}\left(\frac{n_x}{a}\right)^2 E_m; b_{19} = -\frac{n_x}{a}E_m. \quad \text{(A5)}$$

$$c_1 = b_1 - b_7a_5; c_2 = b_2 - b_7a_8; c_3 = b_3; c_4 = b_4 + b_6a_1 + b_7a_2a_1; c_5 = b_5 + b_6a_2 + b_7a_1 + b_7a_2a_2;$$

$$c_6 = b_8; c_7 = b_9 + b_6a_3 + b_7a_2a_3; c_8 = b_{10} + b_6a_4 + b_7a_3 + b_7a_2a_4; c_9 = b_{11} + b_6a_5 + b_7a_4 + b_7a_2a_5$$

$$c_{10} = b_{12}; c_{11} = b_{13} + b_6a_6 + b_7a_2a_6; c_{12} = b_{14} + b_6a_7 + b_7a_6 + b_7a_2a_7; c_{13} = b_{15} + b_6a_8 + b_7a_7 + b_7a_2a_8$$

$$c_{14} = b_{16} + b_6a_9 + b_7a_2a_9; c_{15} = b_{17} + b_6a_{10} + b_7a_9 + b_7a_2a_{10}; c_{16} = b_{18} + b_7a_{10}; c_{17} = b_{19} \quad \text{(A6)}$$

$$d_1 = D_{11}^s + \frac{1}{2}\left(A_m + B_m\right); d_2 = H_{11} + \frac{1}{4}\left(A_m + 2B_m + C_m\right); d_3 = \frac{1}{4}\left(E_m + D_m\right); d_4 = \frac{n_x}{a}J_1\omega^2;$$

$$d_5 = \left(\frac{n_x}{a}\right)^2 B_{11}^s + J_1\omega^2; d_6 = 2\frac{n_x}{a}B_{11}^s; d_7 = B_{11}^s; d_8 = I_0\omega^2; d_9 = -\frac{n_x}{a}J_2\omega^2;$$

$$d_{10} = -\left(\frac{n_x}{a}\right)^2\left[D_{11}^s + \frac{1}{2}\left(A_m + B_m\right)\right] - J_2\omega^2; d_{11} = -\frac{n_x}{a}\left[2D_{11}^s + \left(A_m + B_m\right)\right]; d_{12} = I_0\omega^2;$$

$$d_{13} = \frac{n_x}{a}\left(A_{55}^s + \frac{1}{4}H_m - K_2\omega^2\right); d_{14} = A_{55}^s - \left(\frac{n_x}{a}\right)^2 H_{11} - \frac{1}{4}\left(\frac{n_x}{a}\right)^2\left(A_m + 2B_m + C_m\right) + \frac{1}{4}H_m - K_2\omega^2;$$

$$d_{15} = -2\frac{n_x}{a}H_{11} - \frac{1}{2}\frac{n_x}{a}\left(A_m + 2B_m + C_m\right); d_{16} = \left(\frac{n_x}{a}\right)^2 L_{13}^s + J_0\omega^2; d_{17} = 2\frac{n_x}{a}L_{13}^s + \frac{n_x}{a}A_{55}^s - \frac{1}{4}\frac{n_x}{a}H_m;$$

$$d_{18} = L_{13}^s + A_{55}^s - \frac{1}{4}\left(\frac{n_x}{a}\right)^2\left(E_m + D_m\right) - \frac{1}{4}H_m; d_{19} = -\frac{1}{2}\frac{n_x}{a}\left(E_m + D_m\right); \quad \text{(A7)}$$

$$e_1 = d_1 - d_7a_5; e_2 = d_2 - d_7a_8; e_3 = d_3; e_4 = d_4 + d_6a_1 + d_7a_2a_1; e_5 = d_5 + d_6a_2 + d_7a_1 + d_7a_2a_2;$$

$$e_6 = d_8; e_7 = d_9 + d_6a_3 + d_7a_2a_3; e_8 = d_{10} + d_6a_4 + d_7a_3 + d_7a_2a_4; e_9 = d_{11} + d_6a_5 + d_7a_4 + d_7a_2a_5;$$

$$e_{10} = d_{12}; e_{11} = d_{13} + d_6a_6 + d_7a_2a_6; e_{12} = d_{14} + d_6a_7 + d_7a_6 + d_7a_2a_7; e_{13} = d_{15} + d_6a_8 + d_7a_7 + d_7a_2a_8;$$

$$e_{14} = d_{16} + d_6a_9 + d_7a_2a_9; e_{15} = d_{17} + d_6a_{10} + d_7a_9 + d_7a_2a_{10}; e_{16} = d_{18} + d_7a_{10}; e_{17} = d_{19}. \quad \text{(A8)}$$

$$f_1 = \frac{1}{2}E_m; f_2 = \frac{1}{4}\left(E_m + D_m\right); f_3 = \frac{1}{4}F_m; f_4 = -K_{13}; f_5 = J_0\omega^2; f_6 = L_{13} - \frac{1}{2}\left(\frac{n_x}{a}\right)^2 E_m; f_7 = -\frac{n_x}{a}E_m;$$

$$f_8 = J_0\omega^2; f_9 = \frac{n_x}{a}A_{55}^s + \frac{1}{4}\frac{n_x}{a}H_m; f_{10} = L_{13}^s + A_{55}^s + \frac{1}{4}H_m - \frac{1}{4}\left(\frac{n_x}{a}\right)^2\left(E_m + D_m\right); f_{11} = -\frac{1}{2}\frac{n_x}{a}\left(E_m + D_m\right);$$

$$f_{12} = -Z_{33} + K_0\omega^2; f_{13} = \frac{n_x}{a} A_{55}^s - \frac{1}{4}\frac{n_x}{a} H_m; f_{14} = A_{55}^s - \frac{1}{4} H_m - \frac{1}{4}\left(\frac{n_x}{a}\right)^2 F_m; f_{15} = -\frac{1}{2}\frac{n_x}{a} F_m; \quad \text{(A9)}$$

Figure Captions

Fig. 1: Coordinate and variation of Young's modulus in BDFG beams.

Fig. 2: Vibration mode shapes of SiC/Al microbeams $\left(C-C, a/h=5, h/l=2, n_z=2\right)$ using HOBT and quasi-3D theory.

Fig. 3: Variation of natural frequencies $\bar{\Omega}$ with respect to the power-law index n_z $\left(\text{SiC/Al beams}, a/h=5,\ h/l=2\right)$.

Fig. 4: Vibration mode shapes of immovable and movable simply supported SiC/Al microbeams $\left(a/h=5, n_z=2, h/l=2\right)$.

Fig. 5: Variation of mode shapes with respect to the frequencies $\bar{\Omega}$ (SiC/Al beams, $a/h=10,\ n_z=2$).

Fig. 6: Variation of fundamental frequencies of BDFG micro-beams $\left(a/h=20, h/l=2\right)$ with respect to exponential-indices.

Fig. 7: Difference between Type B and Type C in BDFG beams $\left(a/h=5\right)$.

Fig. 8: Effect of the left and right ends to the frequencies of BDFG beams $\left(a/h=5, n_z=1\right)$.

Fig. 9: Effect of the axial exponential index to the vibration mode shapes of BDFG beams $\left(a/h=5, h/l=2, n_z=2\right)$.

Table Captions

Table 1: Comparisons of non-dimensional natural frequencies $\tilde{\Omega}$ of SiC/Al microbeams for various h/l $\left(a/h=12, n_z=2\right)$.

Table 2: Size effect of frequencies $\bar{\Omega}$ for the SiC/Al beams under various BCs and slenderness ratios.

Table 3: Fundamental frequencies of C-C BDFG beams $\left(a/h=5\right)$.

Table 4: Fundamental frequencies of C-S BDFG beams $\left(a/h=5\right)$.

Table 5: Fundamental frequencies of S-S BDFG beams $\left(a/h=5\right)$.

Table 6: Fundamental frequencies of C-F BDFG beams $\left(a/h=5\right)$.

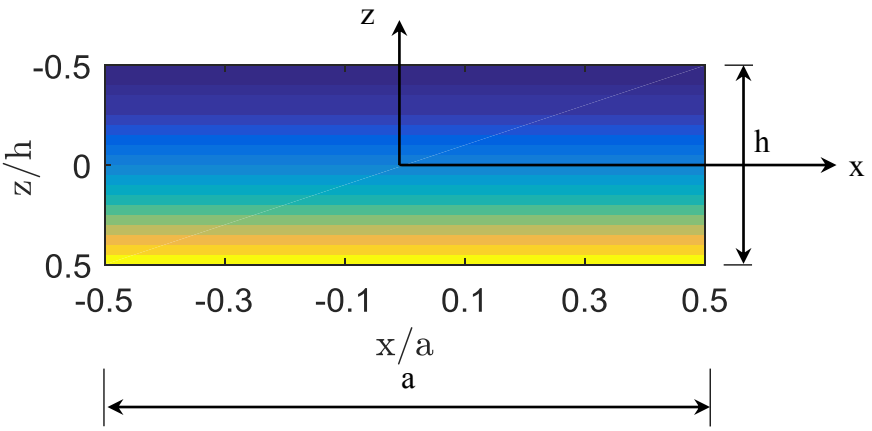

a. Type A $(n_x = 0, n_z = 2)$

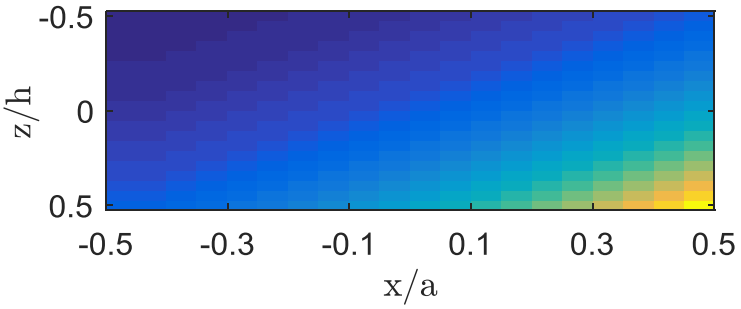

b. Type B $(n_x = 2, n_z = 2)$

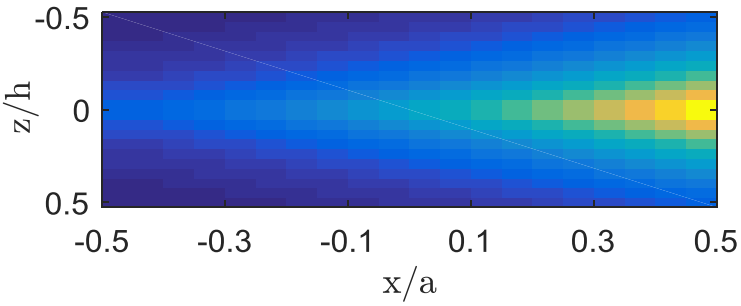

c. Type C $(n_x = 2, n_z = 2)$

Fig. 1: Coordinate and variation of Young's modulus in BDFG beams.

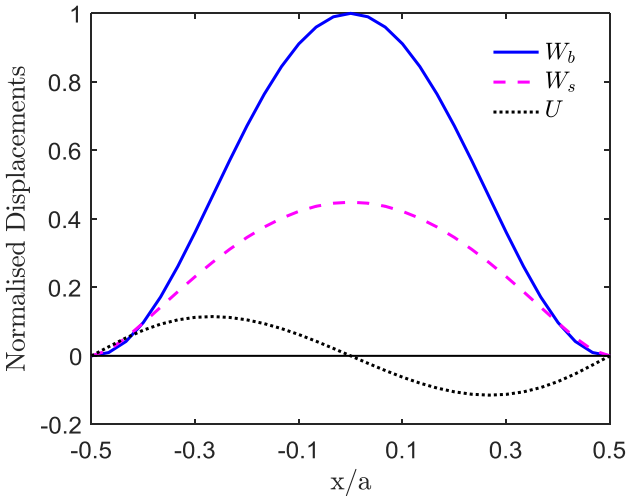

Mode 1: $\bar{\Omega}_1 = 13.2810$

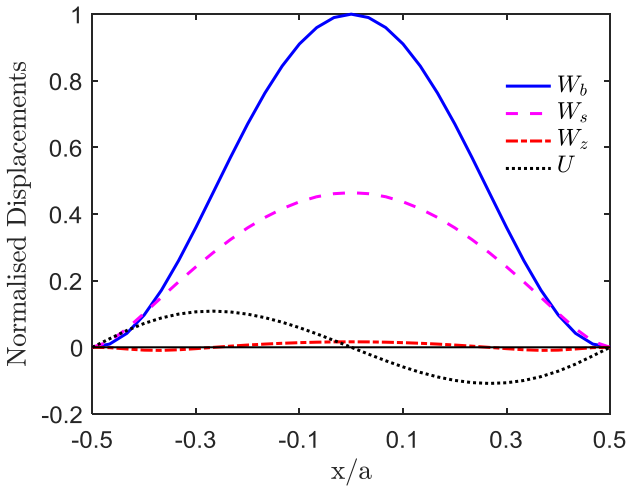

Mode 1: $\bar{\Omega}_1 = 13.3446$

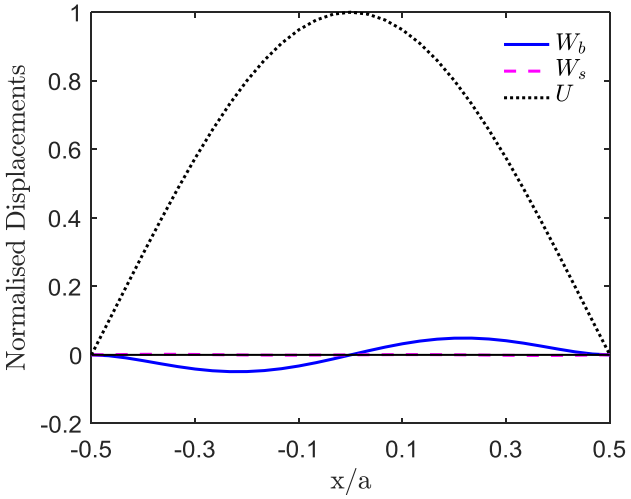

Mode 2: $\bar{\Omega}_2 = 25.1587$

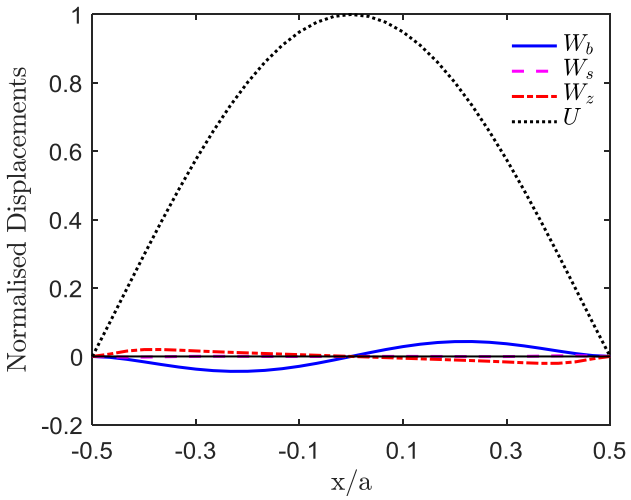

Mode 2: $\bar{\Omega}_2 = 25.8440$

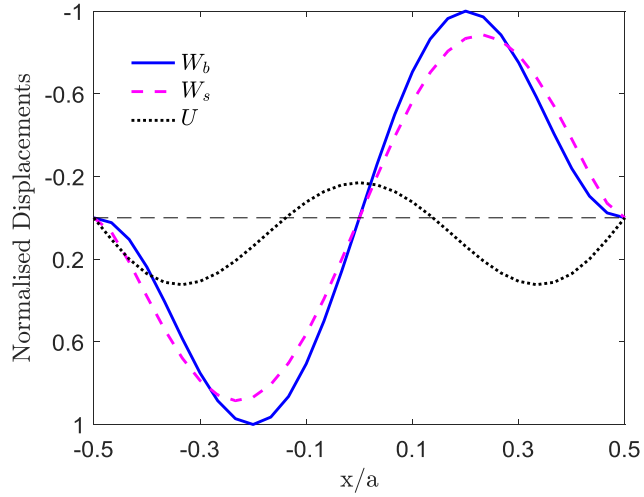

Mode 3: $\bar{\Omega}_3 = 33.6027$

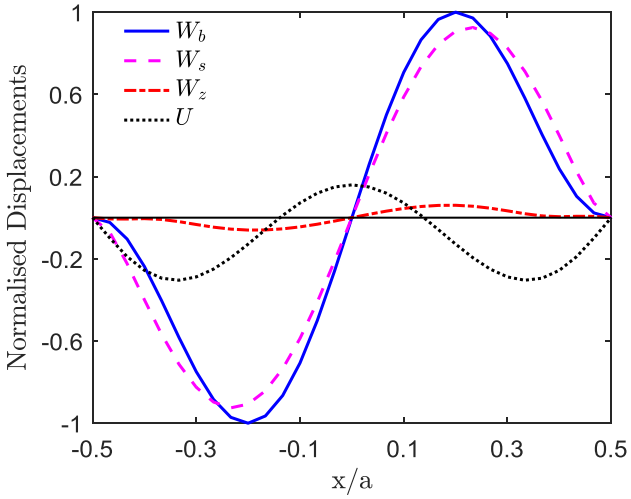

Mode 3: $\bar{\Omega}_3 = 33.6035$

a. HOBT

b. Quasi-3D

Fig. 2: Vibration mode shapes of SiC/Al microbeams $(C-C, a/h=5, h/l=2, n_z=2)$ using HOBT and quasi-3D theory.

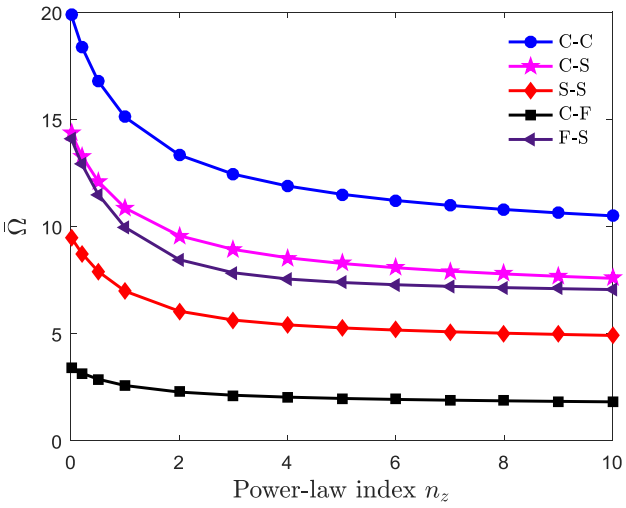

Fig. 3: Variation of natural frequencies $\bar{\Omega}$ with respect to the power-law index n_z $\left(\text{SiC/Al beams}, a/h=5,\ \ h/l=2\right)$.

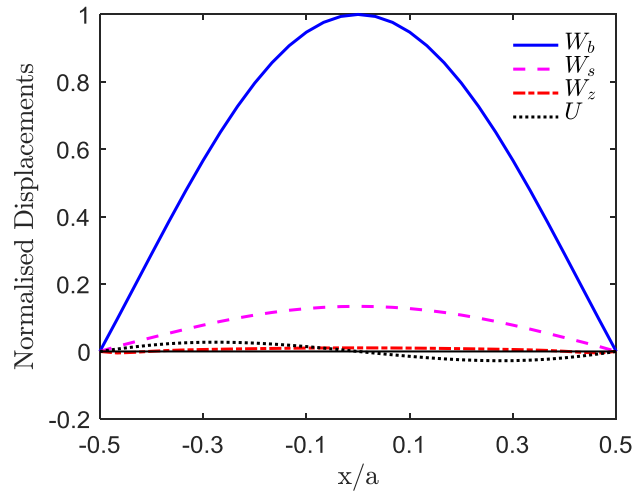

Mode 1: $\bar{\Omega}_1 = 7.3804$

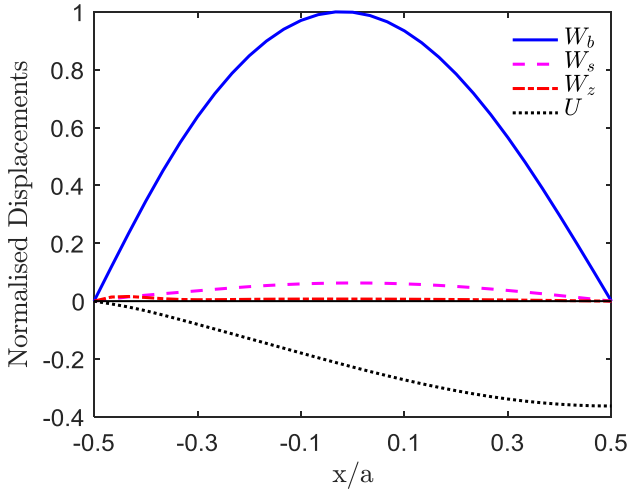

Mode 1: $\bar{\Omega}_1 = 6.0555$

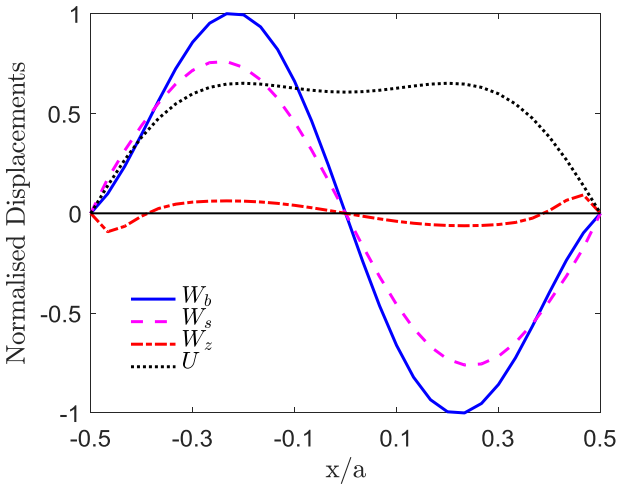

Mode 2: $\bar{\Omega}_2 = 18.8083$

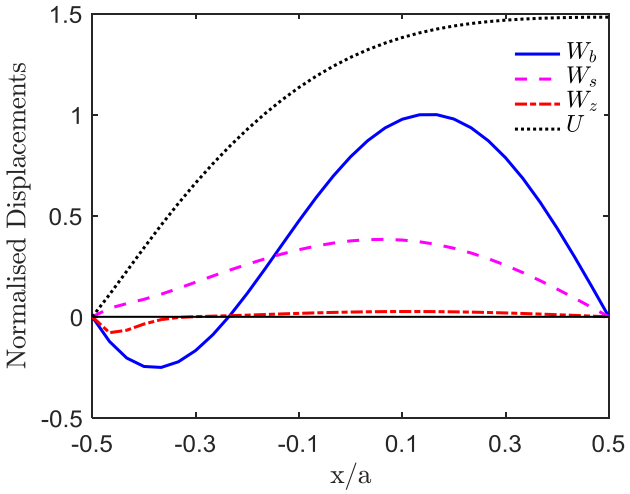

Mode 2: $\bar{\Omega}_2 = 12.4521$

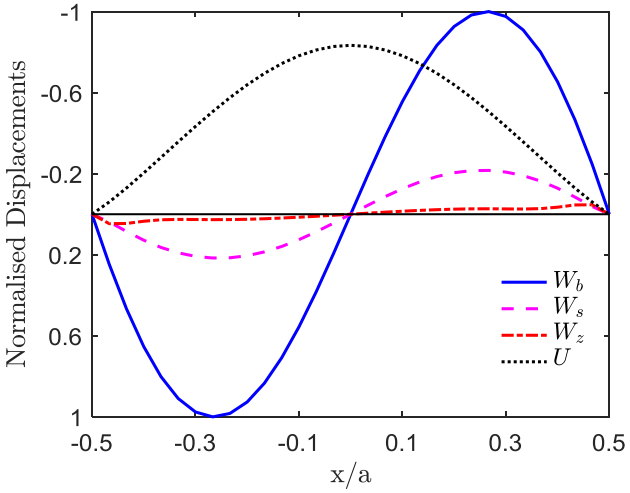

Mode 3: $\bar{\Omega}_3 = 29.2417$

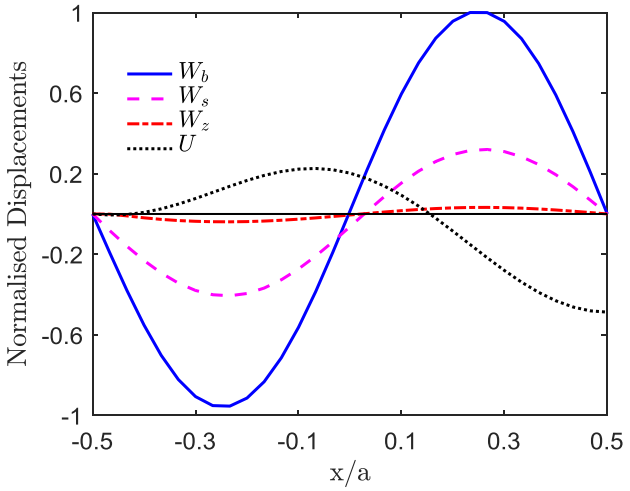

Mode 3: $\bar{\Omega}_3 = 23.1669$

a. Immovable SS beams

b. Movable SS beams

Fig. 4: Vibration mode shapes of immovable and movable simply supported SiC/Al microbeams $(a/h = 5, n_z = 2, h/l = 2)$.

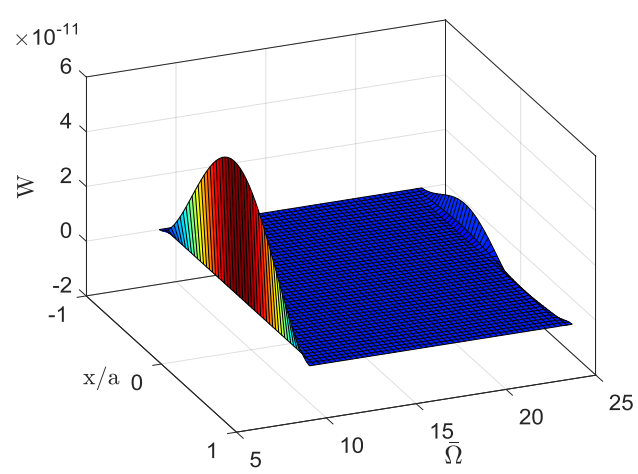

$h/l=\infty$

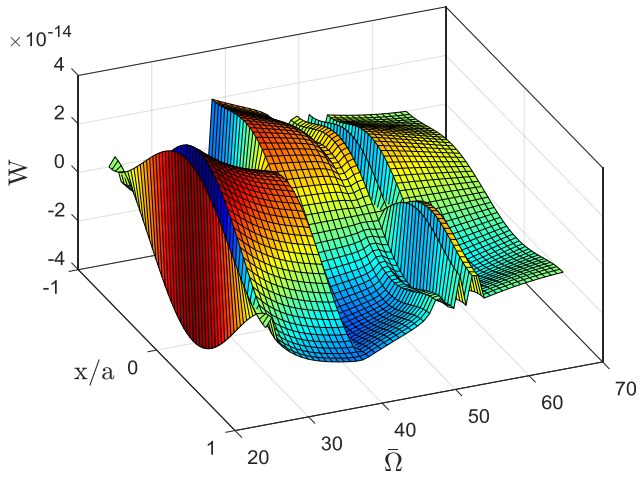

$h=l$

a. C-C beams

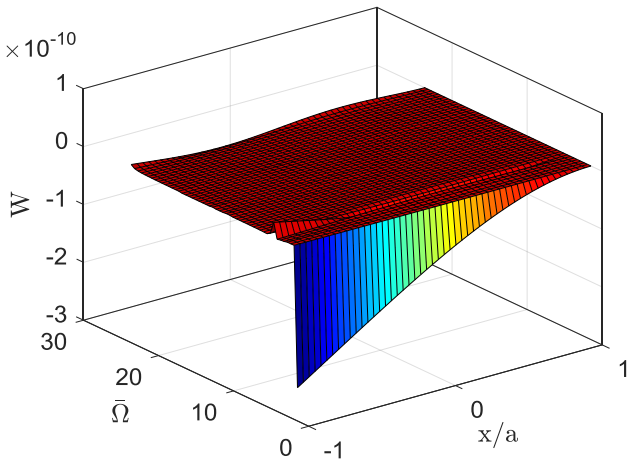

$h/l=\infty$

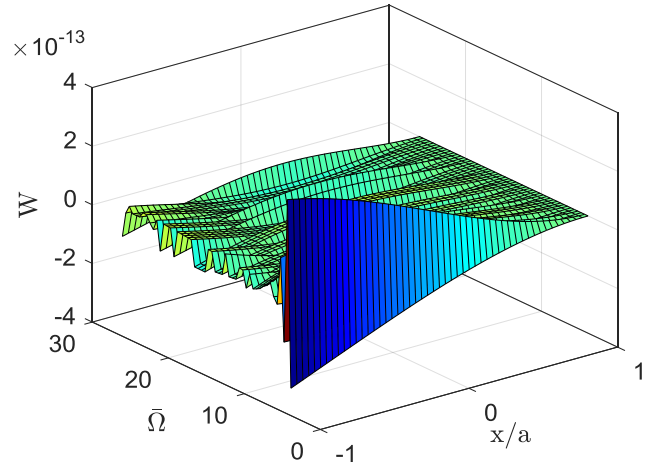

$h=l$

b. F-C beams

Fig. 5: Variation of mode shapes with respect to the frequencies $\bar{\Omega}$ (SiC/Al beams, $a/h=10$, $n_z=2$).

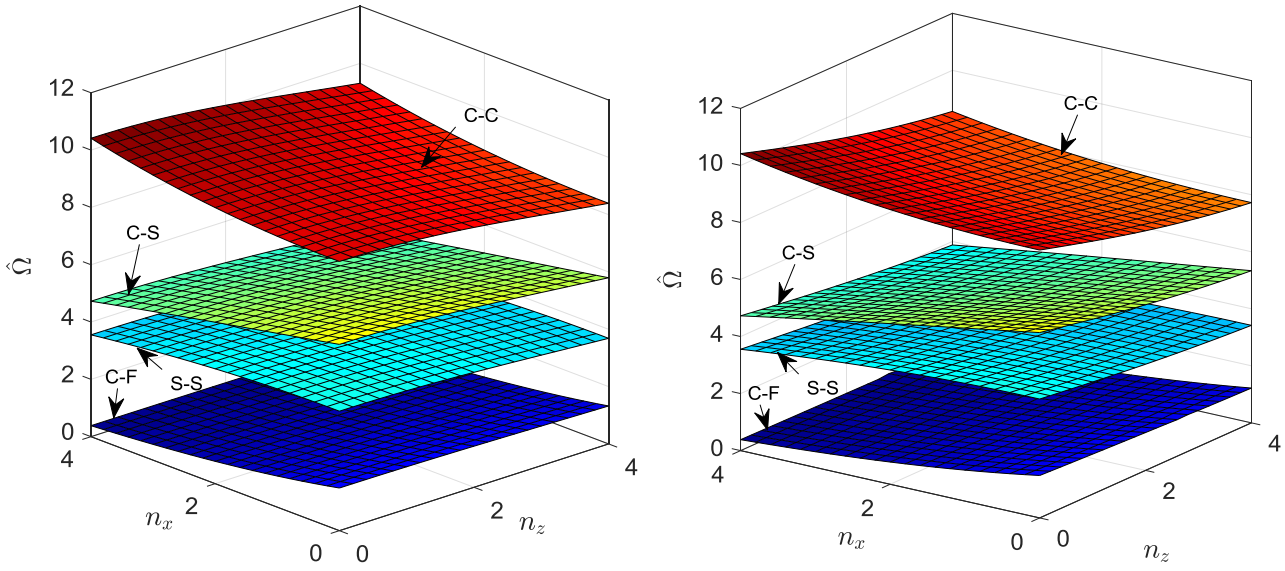

Type B Type C

Fig. 6: Variation of fundamental frequencies of BDFG micro-beams $(a/h = 20, h/l = 2)$ with respect to exponential-indices.

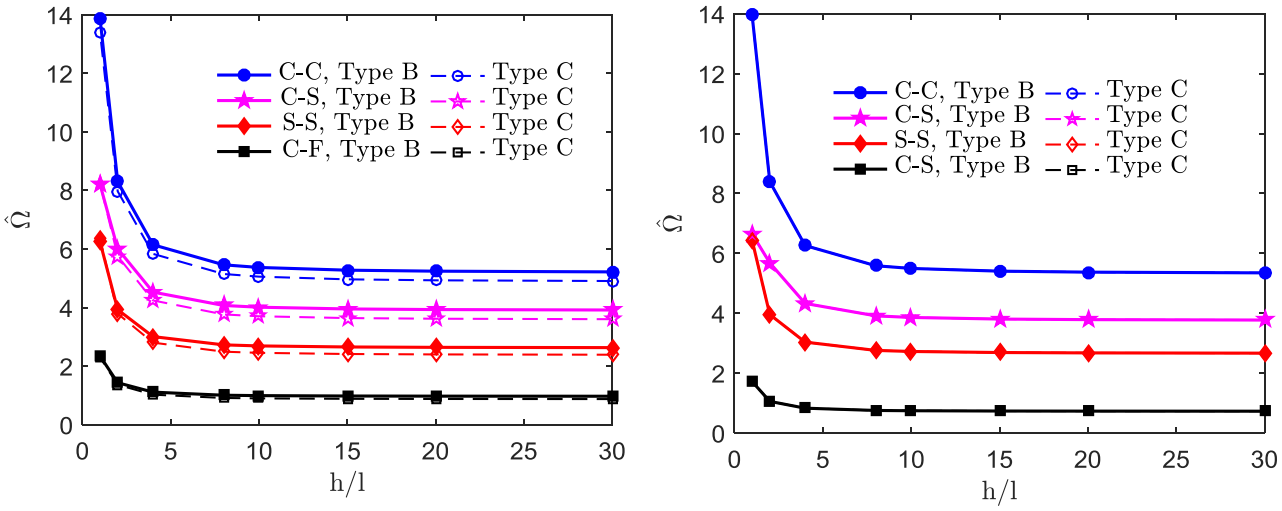

a. Through-the-thickness FG (n_x=0, n_z=1) b. Axial FG (n_x=1, n_z=0)

Fig. 7: Difference between Type B and Type C in BDFG beams $(a/h=5)$.

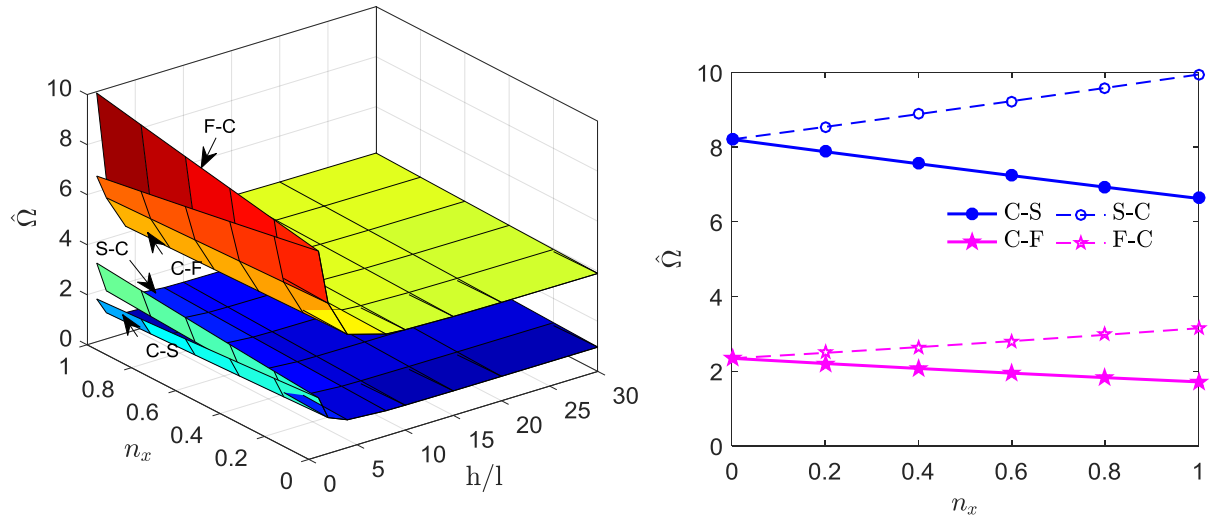

a. $\hat{\Omega}-n_x-h/l$ b. $\hat{\Omega}-n_x\left(h/l=1\right)$

Fig. 8: Effect of the left and right ends to the frequencies of BDFG beams $\left(a/h=5,n_z=1\right)$.

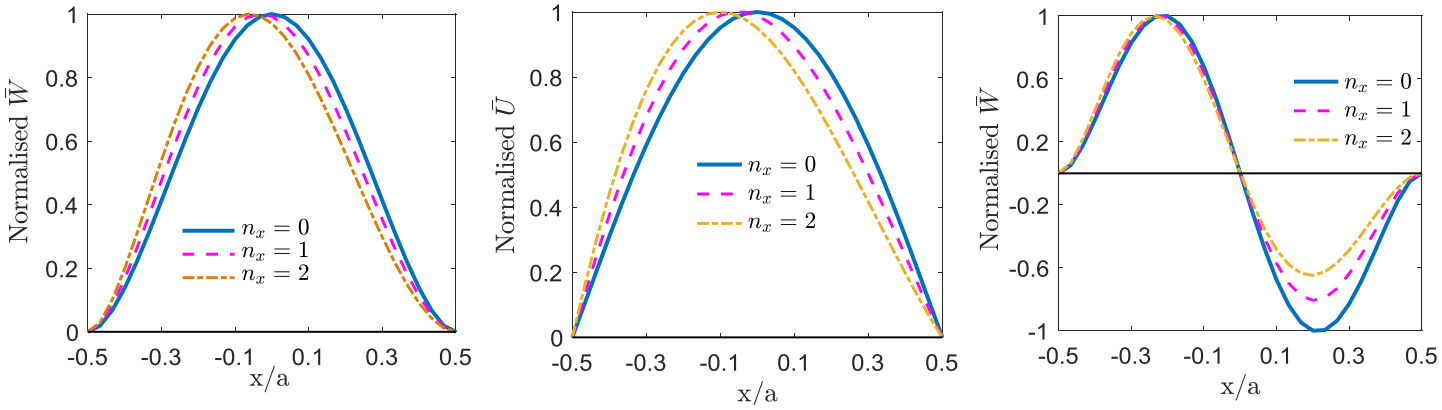

Mode 1 Mode 2 Mode 3

a. C-C beams

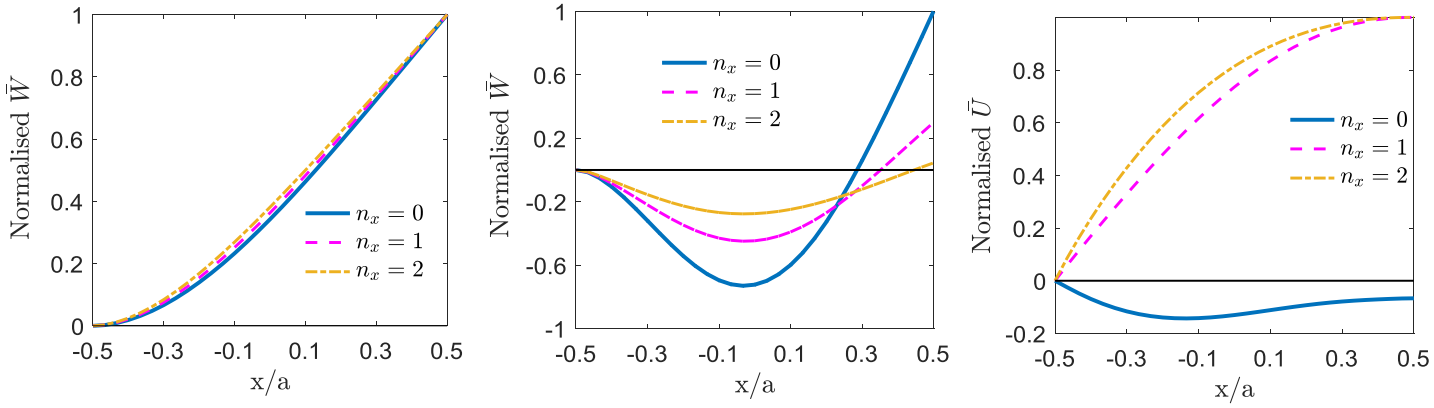

Mode 1 Mode 2(i) Mode 2(ii)

b. C-F beams

Fig. 9: Effect of the axial exponential index to the vibration mode shapes of BDFG beams $(a/h = 5, h/l = 2, n_z = 2)$.

Table 1: Comparisons of non-dimensional natural frequencies $\tilde{\Omega}$ of SiC/Al microbeams for various h/l $\left(a/h=12, n_z=2\right)$.

BCs	Theory	h/l					
		1	1.5	2	3	6	10
C–C	HOBT [72]	1.6246	1.2291	1.0642	0.8904	0.7769	0.7454
	FOBT [12]	1.6022	1.2194	1.0416	0.8885	0.7801	0.7548
	HOBT	1.6892	1.2522	1.0565	0.8896	0.7709	0.7427
	Quasi-3D	1.6762	1.2355	1.0373	0.8676	0.7461	0.7171
S–S	HOBT [72]	0.7854	0.5903	0.5042	0.4304	0.3787	0.3662
	FOBT [12]	0.7625	0.5784	0.4968	0.4285	0.3812	0.3701
	HOBT	0.7664	0.5777	0.4948	0.4255	0.3777	0.3666
	Quasi-3D	0.8256	0.6131	0.5145	0.4284	0.3663	0.3517
C-S	HOBT	1.1756	0.8759	0.7426	0.6299	0.5508	0.5323
	Quasi-3D	1.1810	0.8743	0.7355	0.6165	0.5318	0.5118
C-F	HOBT	0.2695	0.2008	1.0426	0.1447	0.1268	0.1227
	Quasi-3D	0.2671	0.1976	0.1666	0.1397	0.1220	0.1177
F-S	HOBT	1.1653	0.8683	0.7361	0.6245	0.5464	0.5282
	Quasi-3D	1.1322	0.8451	0.7140	0.5961	0.5251	0.5062

Table 2: Size effect of frequencies $\bar{\Omega}$ for the SiC/Al beams under various BCs and slenderness ratios.

BCs	h/l	Theory	a/h=5			a/h=20		
			n_z=0	1	10	n_z=0	1	10
S_1-S_1	1	HOBT [42]	15.7140	11.9948	8.0425	-	-	-
		HOBT	15.7140	12.1506	8.1733	16.2251	12.5446	8.4065
		Quasi-3D [42]	15.6249	11.9444	7.9967	-	-	-
		Quasi-3D	15.6833	9.3951	3.9212	16.2228	13.7186	8.9625
S_1-S_2		HOBT	15.7140	11.7745	7.8469	16.2251	12.3911	8.2843
		Quasi-3D	15.6833	9.4005	7.4030	16.2228	12.3681	8.2808
S_1-S_1	5	HOBT	6.8405	5.2905	3.9046	7.1862	5.5598	4.1859
		Quasi-3D	6.8427	5.4276	3.9412	7.1864	5.7077	4.2296
S_1-S_2		HOBT	6.8405	4.9615	3.6775	7.1862	5.2255	3.9508
		Quasi-3D	6.8427	4.9893	3.7046	7.1864	5.2631	3.9827
S_1-S_1	∞	HOBT [42]	6.2025	4.4657	3.3909	-	-	-
		HOBT	6.2009	4.7944	3.6022	6.5441	5.0618	3.9102
		Quasi-3D [42]	6.4615	4.7159	3.5444	-	-	-
		Quasi-3D	6.2069	4.8119	3.6146	6.5445	5.0758	3.9215
S_1-S_2		HOBT	6.2009	4.4404	3.3692	6.5441	4.6954	3.6596
		Quasi-3D	6.2069	4.4865	3.4052	6.5445	4.7382	3.6945
C-C	1	HOBT	33.5290	25.7024	17.4627	36.5871	27.9617	18.7167
		Quasi-3D	33.5390	25.7114	17.4235	36.5928	28.0028	18.7560
	5	HOBT	13.8093	10.2076	7.2212	16.1273	11.7461	8.8328
		Quasi-3D	13.8604	10.3089	7.3016	16.1437	11.8454	8.9182
	∞	HOBT	12.2556	8.9576	6.3403	14.6657	10.5412	8.1522
		Quasi-3D	12.3018	9.0664	6.4268	14.6811	10.6488	8.2419
C-S	1	HOBT	18.1099	14.2757	9.4339	25.2986	19.3299	12.9292
		Quasi-3D	18.3774	14.6234	9.7854	25.2990	19.3553	12.9531
	5	HOBT	10.2151	7.4889	5.4437	11.1866	8.1408	6.1434
		Quasi-3D	10.2396	7.5569	5.4968	11.1924	8.2050	6.1980
	∞	HOBT	9.1925	6.6568	4.9064	10.1823	7.3118	5.6836
		Quasi-3D	9.2208	6.7343	4.9679	10.1879	7.3823	5.7417
C-F	1	HOBT	5.6973	4.3504	2.9127	5.7873	4.4215	2.9559
		Quasi-3D	5.6756	4.3425	2.9191	5.7864	4.4269	2.9622
	5	HOBT	2.5043	1.8236	1.3667	2.5649	1.8655	1.4117
		Quasi-3D	2.5102	1.8425	1.3873	2.5661	1.8804	1.4246
	∞	HOBT	2.2769	1.6362	1.2604	2.3361	1.6765	1.3082
		Quasi-3D	2.2804	1.6544	1.2761	2.3371	1.6926	1.3215
S-F	1	HOBT	18.1099	13.8537	9.1175	25.2960	19.3008	12.9008
		Quasi-3D	18.3774	12.8911	8.8361	25.2718	19.1880	12.8636
	5	HOBT	10.3774	7.4181	5.4633	11.2015	8.1390	6.1505
		Quasi-3D	10.3936	7.4632	5.5363	11.2030	8.1981	6.2029
	∞	HOBT	9.3982	6.6424	5.0073	10.2001	7.3130	5.6963
		Quasi-3D	9.4119	6.7241	5.0785	10.2012	7.3805	5.7517

Table 3: Fundamental frequencies of C-C BDFG beams $(a/h=5)$.

h/l	n_x	Theory	Type B				Type C			
			n_z=0	0.4	0.6	1	n_z=0	0.4	0.6	1
1	0	HOBT	13.8706	13.8720	13.8737	13.8787	13.8706	13.6821	13.5876	13.3996
		Quasi-3D	13.8581	13.8612	13.8650	13.8761	13.8581	13.6680	13.5728	13.3838
	0.4	HOBT	13.8854	13.8868	13.8885	13.8935	13.8854	13.6969	13.6024	13.4143
		Quasi-3D	13.8730	13.8761	13.8798	13.8910	13.8730	13.6829	13.5876	13.3987
	0.6	HOBT	13.9039	13.9053	13.9070	13.9119	13.9039	13.7155	13.6209	13.4328
		Quasi-3D	13.8916	13.8947	13.8984	13.9095	13.8916	13.7015	13.6062	13.4172
	1	HOBT	13.9634	13.9647	13.9664	13.9712	13.9634	13.7749	13.6802	13.4922
		Quasi-3D	13.9513	13.9544	13.9581	13.9690	13.9513	13.7611	13.6658	13.4768
8	0	HOBT	5.4880	5.4711	5.4502	5.3846	5.4880	5.3463	5.2674	5.0963
		Quasi-3D	5.5438	5.5303	5.5135	5.4604	5.5438	5.4003	5.3204	5.1468
	0.4	HOBT	5.4947	5.4778	5.4569	5.3912	5.4947	5.3527	5.2737	5.1023
		Quasi-3D	5.5505	5.5370	5.5201	5.4670	5.5505	5.4068	5.3267	5.1527
	0.6	HOBT	5.5031	5.4862	5.4652	5.3994	5.5031	5.3607	5.2815	5.1097
		Quasi-3D	5.5589	5.5453	5.5285	5.4752	5.5589	5.4148	5.3345	5.1602
	1	HOBT	5.5299	5.5129	5.4919	5.4257	5.5299	5.3864	5.3066	5.1335
		Quasi-3D	5.5857	5.5720	5.5551	5.5015	5.5857	5.4404	5.3595	5.1840
∞	0	CBT [58]	6.3291	6.3056	6.2763	6.1826	-	-	-	-
		FOBT [58]	5.1943	5.1806	5.1630	5.1083	-	-	-	-
		HOBT	5.2308	5.2128	5.1904	5.1202	5.2308	5.0907	5.0110	4.8351
		Quasi-3D	5.2869	5.2725	5.2546	5.1981	5.2869	5.1453	5.0646	4.8865
	0.4	CBT [58]	6.3349	6.3115	6.2822	6.1884	-	-	-	-
		FOBT [58]	5.1982	5.1845	5.1669	5.1123	-	-	-	-
		HOBT	5.2374	5.2193	5.1970	5.1266	5.2374	5.0969	5.0171	4.8409
		Quasi-3D	5.2935	5.2791	5.2612	5.2046	5.2935	5.1515	5.0707	4.8923
	0.6	CBT [58]	6.3427	6.3193	6.288	6.1943	-	-	-	-
		FOBT [58]	5.2041	5.1904	5.1728	5.1181	-	-	-	-
		HOBT	5.2456	5.2275	5.2051	5.1347	5.2456	5.1048	5.0247	4.8481
		Quasi-3D	5.3017	5.2873	5.2693	5.2127	5.3017	5.1594	5.0783	4.8995
	1	CBT [58]	6.3662	6.3427	6.3115	6.2177	-	-	-	-
		FOBT [58]	5.2197	5.2060	5.1884	5.1337	-	-	-	-
		HOBT	5.2719	5.2538	5.2312	5.1604	5.2719	5.1298	5.0491	4.8711
		Quasi-3D	5.3280	5.3135	5.2954	5.2384	5.3280	5.1844	5.1027	4.9225

Table 4: Fundamental frequencies of C-S BDFG beams $(a/h=5)$.

h/l	n_x	Theory	Type B				Type C			
			n_z=0	0.4	0.6	1	n_z=0	0.4	0.6	1
1	0	HOBT	7.8540	7.8540	7.8540	7.8540	7.8540	7.8540	7.8540	7.8540
		Quasi-3D	8.2332	8.2289	8.2236	8.2075	8.2332	8.2332	8.2332	8.2332
	0.4	HOBT	7.2297	7.2297	7.2297	7.2297	7.2297	7.2297	7.2297	7.2297
		Quasi-3D	7.5787	7.5748	7.5700	7.5553	7.5787	7.5787	7.5787	7.5787
	0.6	HOBT	6.9270	6.9270	6.9270	6.9270	6.9270	6.9270	6.9270	6.9270
		Quasi-3D	7.2614	7.2577	7.2531	7.2392	7.2614	7.2614	7.2614	7.2614
	1	HOBT	6.3414	6.3414	6.3414	6.3414	6.3414	6.3414	6.3414	6.3414
		Quasi-3D	6.6476	6.6442	6.6401	6.6274	6.6476	6.6476	6.6476	6.6476
8	0	HOBT	4.1147	4.1011	4.0843	4.0315	4.1147	3.9743	3.8998	3.7443
		Quasi-3D	4.1406	4.1294	4.1154	4.0714	4.1406	3.9985	3.9231	3.7657
	0.4	HOBT	4.0229	4.0096	3.9931	3.9413	4.0229	3.8834	3.8096	3.6559
		Quasi-3D	4.0484	4.0373	4.0236	3.9803	4.0484	3.9071	3.8324	3.6769
	0.6	HOBT	3.9777	3.9645	3.9481	3.8968	3.9777	3.8386	3.7651	3.6122
		Quasi-3D	4.0029	3.9920	3.9783	3.9354	4.0029	3.8621	3.7877	3.6330
	1	HOBT	3.8878	3.8748	3.8588	3.8085	3.8878	3.7494	3.6765	3.5254
		Quasi-3D	3.9125	3.9017	3.8883	3.8460	3.9125	3.7724	3.6986	3.5456
∞	0	CBT [58]	4.3682	4.3511	4.3304	4.2657	-	-	-	-
		FOBT [58]	3.8779	3.8662	3.8505	3.8037	-	-	-	-
		HOBT	3.9502	3.9359	3.9182	3.8626	3.9502	3.8068	3.7299	3.5680
		Quasi-3D	3.9775	3.9657	3.9510	3.9047	3.9775	3.8321	3.7543	3.5903
	0.4	CBT [58]	4.2486	4.2315	4.2120	4.1485	-	-	-	-
		FOBT [58]	3.7685	3.7568	3.7431	3.6962	-	-	-	-
		HOBT	3.8633	3.8493	3.8320	3.7775	3.8633	3.7207	3.6445	3.4844
		Quasi-3D	3.8902	3.8786	3.8642	3.8186	3.8902	3.7456	3.6684	3.5063
	0.6	CBT [58]	4.1888	4.1729	4.1522	4.0899	-	-	-	-
		FOBT [58]	3.7138	3.7021	3.6865	3.6416	-	-	-	-
		HOBT	3.8206	3.8067	3.7895	3.7355	3.8206	3.6783	3.6023	3.4431
		Quasi-3D	3.8472	3.8357	3.8214	3.7762	3.8472	3.7029	3.6260	3.4648
	1	CBT [58]	4.0704	4.0545	4.0350	3.9752	-	-	-	-
		FOBT [58]	3.6005	3.5908	3.5751	3.5322	-	-	-	-
		HOBT	3.7357	3.7221	3.7052	3.6523	3.7357	3.5939	3.5185	3.3610
		Quasi-3D	3.7618	3.7505	3.7364	3.6919	3.7618	3.6181	3.5417	3.3821

Table 5: Fundamental frequencies of S-S BDFG beams $\left(a/h=5\right)$.

h/l	n_x	Theory	Type B				Type C			
			n_z=0	0.4	0.6	1	n_z=0	0.4	0.6	1
1	0	HOBT	6.5172	6.5078	6.4963	6.4610	6.5172	6.4593	6.4306	6.3745
		Quasi-3D	6.4944	6.4505	6.3978	6.2432	6.4944	6.4369	6.4086	6.3533
	0.4	HOBT	6.5074	6.4999	6.4907	6.4622	6.5074	6.4497	6.4211	6.3652
		Quasi-3D	6.4846	6.4217	6.3499	6.1546	6.4846	6.4274	6.3991	6.3440
	0.6	HOBT	6.4951	6.4882	6.4797	6.4533	6.4951	6.4377	6.4092	6.3536
		Quasi-3D	6.4724	6.3913	6.3044	6.0833	6.4724	6.4154	6.3873	6.3325
	1	HOBT	6.4558	6.4496	6.4420	6.4184	6.4558	6.3992	6.3712	6.3164
		Quasi-3D	6.4334	6.2597	6.1332	5.8673	6.4334	6.3773	6.3496	6.2956
8	0	HOBT	2.7786	2.7679	2.7546	2.7132	2.7786	2.6672	2.6097	2.4924
		Quasi-3D	2.7820	2.7730	2.7618	2.7266	2.7820	2.6698	2.6119	2.4939
	0.4	HOBT	2.7749	2.7643	2.7511	2.7100	2.7749	2.6636	2.6061	2.4889
		Quasi-3D	2.7783	2.7692	2.7580	2.7225	2.7783	2.6662	2.6083	2.4904
	0.6	HOBT	2.7702	2.7597	2.7466	2.7057	2.7702	2.6590	2.6016	2.4845
		Quasi-3D	2.7736	2.7645	2.7532	2.7176	2.7736	2.6616	2.6038	2.4860
	1	HOBT	2.7554	2.7449	2.7319	2.6914	2.7554	2.6444	2.5871	2.4704
		Quasi-3D	2.7587	2.7495	2.7381	2.7021	2.7587	2.6469	2.5893	2.4719
∞	0	CBT [58]	2.8033	2.7911	2.7764	2.7288	-	-	-	-
		FOBT [58]	2.6767	2.6669	2.6533	2.6103	-	-	-	-
		HOBT	2.6774	2.6663	2.6525	2.6096	2.6774	2.5622	2.5024	2.3798
		Quasi-3D	2.6820	2.6728	2.6613	2.6253	2.6820	2.5658	2.5055	2.3820
	0.4	CBT [58]	2.7984	2.7862	2.7716	2.7239	-	-	-	-
		FOBT [58]	2.6728	2.6611	2.6474	2.6044	-	-	-	-
		HOBT	2.6738	2.6628	2.6492	2.6066	2.6738	2.5587	2.4990	2.3764
		Quasi-3D	2.6784	2.6692	2.6577	2.6214	2.6784	2.5623	2.5021	2.3787
	1	CBT [58]	2.7740	2.7618	2.7471	2.6983	-	-	-	-
		FOBT [58]	2.6455	2.6337	2.6201	2.5771	-	-	-	-
		HOBT	2.6552	2.6444	2.6309	2.5889	2.6552	2.5404	2.4809	2.3589
		Quasi-3D	2.6597	2.6504	2.6388	2.6022	2.6597	2.5440	2.4840	2.3611

Table 6: Fundamental frequencies of C-F BDFG beams $(a/h=5)$.

h/l	n_x	Theory	Type B				Type C			
			n_z=0	0.4	0.6	1	n_z=0	0.4	0.6	1
1	0	HOBT	2.3640	2.3625	2.3605	2.3544	2.3640	2.3433	2.3331	2.3132
		Quasi-3D	2.3513	2.3502	2.3488	2.3445	2.3513	2.3295	2.3188	2.2977
	0.4	HOBT	2.0912	2.0897	2.0879	2.0824	2.0912	2.0728	2.0638	2.0462
		Quasi-3D	2.0788	2.0778	2.0766	2.0727	2.0788	2.0595	2.0500	2.0313
	0.6	HOBT	1.9646	1.9632	1.9616	1.9563	1.9646	1.9473	1.9389	1.9224
		Quasi-3D	1.9525	1.9515	1.9504	1.9467	1.9525	1.9344	1.9254	1.9079
	1	HOBT	1.7303	1.7291	1.7275	1.7228	1.7303	1.7151	1.7076	1.6932
		Quasi-3D	1.7187	1.7178	1.7168	1.7135	1.7187	1.7027	1.6948	1.6793
8	0	HOBT	1.0210	1.0172	1.0126	0.9980	1.0210	0.9765	0.9539	0.9081
		Quasi-3D	1.0267	1.0235	1.0194	1.0067	1.0267	0.9820	0.9592	0.9132
	0.4	HOBT	0.9040	0.9006	0.8965	0.8835	0.9040	0.8644	0.8442	0.8035
		Quasi-3D	0.9094	0.9065	0.9029	0.8915	0.9094	0.8695	0.8492	0.8083
	0.6	HOBT	0.8497	0.8465	0.8426	0.8304	0.8497	0.8123	0.7933	0.7550
		Quasi-3D	0.8548	0.8521	0.8487	0.8380	0.8548	0.8172	0.7981	0.7596
	1	HOBT	0.7489	0.7461	0.7427	0.7319	0.7489	0.7158	0.6990	0.6651
		Quasi-3D	0.7538	0.7513	0.7483	0.7389	0.7538	0.7204	0.7035	0.6694
∞	0	CBT [58]	1.0068	1.0029	0.999	0.9833	-	-	-	-
		FOBT [58]	0.9844	0.9796	0.9735	0.9576	-	-	-	-
		HOBT	0.9854	0.9815	0.9766	0.9615	0.9854	0.9392	0.9156	0.8678
		Quasi-3D	0.9902	0.9869	0.9827	0.9695	0.9902	0.9439	0.9202	0.8723
	0.4	CBT [58]	0.8896	0.8876	0.8818	0.8681	-	-	-	-
		FOBT [58]	0.8709	0.8673	0.8624	0.8486	-	-	-	-
		HOBT	0.8725	0.8690	0.8647	0.8512	0.8725	0.8314	0.8104	0.7679
		Quasi-3D	0.8771	0.8741	0.8704	0.8586	0.8771	0.8358	0.8147	0.7721
	1	CBT [58]	0.7353	0.7333	0.7294	0.7177	-	-	-	-
		FOBT [58]	0.7216	0.7177	0.7138	0.7021	-	-	-	-
		HOBT	0.7229	0.7200	0.7164	0.7052	0.7229	0.6885	0.6710	0.6356
		Quasi-3D	0.7271	0.7246	0.7215	0.7116	0.7271	0.6926	0.6750	0.6394